Plane-strain crack problems in microstructured solids governed by dipolar gradient elasticity

P.A. Gourgiotis , H.G. Georgiadis *

Mechanics Division, National Technical University of Athens,
Zographou Campus, Zographou, GR-15773, Greece

Abstract. The present study aims at determining the elastic stress and displacement fields around the tips of a finite-length crack in a microstructured solid under remotely applied plane-strain loading (mode I and II cases). The material microstructure is modeled through the Toupin-Mindlin generalized continuum theory of dipolar gradient elasticity. According to this theory, the strain-energy density assumes the form of a positive-definite function of the strain tensor (as in classical elasticity) and the gradient of the strain tensor (additional term). A simple but yet rigorous version of the theory is employed here by considering an isotropic linear expression of the elastic strain-energy density that involves only three material constants (the two Lamé constants and the so-called gradient coefficient). First, a near-tip asymptotic solution is obtained by the Knein-Williams technique. Then, we attack the complete boundary value problem in an effort to obtain a full-field solution. Hypersingular integral equations with a cubic singularity are formulated with the aid of the Fourier transform. These equations are solved by analytical considerations on Hadamard finite-part integrals and a numerical treatment. The results show significant departure from the predictions of standard fracture mechanics. In view of these results, it seems that the classical theory of elasticity is inadequate to analyze crack problems in microstructured materials. Indeed, the present results indicate that the stress distribution ahead of the crack tip exhibits a local maximum that is bounded.

---

* Corresponding author. Tel.: +30 210 7721365; fax: +30 210 7721302.
E-mail address: georgiad@central.ntua.gr (H.G. Georgiadis).

Therefore, this maximum value may serve as a measure of the critical stress level at which further advancement of the crack may occur. Also, in the vicinity of the crack tip, the crack-face displacement closes more smoothly as compared to the standard result and the strain field is bounded. Finally, the J-integral (energy release rate) in gradient elasticity was evaluated. A decrease of its value is noticed in comparison with the classical theory. This shows that the gradient theory predicts a strengthening effect since a reduction of crack driving force takes place as the material microstructure becomes more pronounced.

Keywords: Cracks; microstructure; dipolar gradient elasticity; asymptotics; hypersingular integral equations.

1. Introduction

It is well known that classical continuum theories possess no intrinsic length scale and thus fail to predict the scale effects observed experimentally in problems with geometric length scales comparable to the lengths of material *microstructure*. On the contrary, generalized continuum theories intend to capture effects of microstructure extending the range of applicability of the 'continuum' concept in an effort to bridge the gap between classical continuum theories and atomic-lattice theories. Notable examples appearing in relatively recent studies include the strengthening effects observed in bending and torsion (Kakunai et al. 1985; Fleck et al., 1994; Stolken and Evans, 1998), the buckling of elastic fibers in composites (Fleck and Shu, 1995), micro-indentation experiments where the measured indentation hardness increases as the width of the indent decreases (Ma and Clarke, 1995; Poole et al., 1996), fracture of cellular materials (Chen et al., 1998), and scale effects in simple structural components (Giannakopoulos and Stamoulis, 2006). An interesting review on experiments in generalized continua is also given by Lakes (1995).

One of the most effective generalized continuum theories proved to be in recent years the theory introduced by Toupin (1962) and Mindlin (1964) – see the brief literature review on applications and extensions, below. The general framework appears under the names 'strain-gradient theory' or 'grade-two theory' or 'dipolar gradient theory'. This approach is appropriate for formulations of both elasticity and plasticity problems and, in general, allows for the emergence of

interesting *boundary layer* effects that can capture corresponding phenomena (see e.g. Shi et al., 2000; Georgiadis, 2003; Georgiadis et al., 2004). In such a formulation, characteristic lengths appear in the mechanical behavior of the material and these lengths can be related with the size of microstructure. Scale effects are incorporated therefore in the stress analysis. Typical cases of continua amenable to such an analysis are periodic material structures like those, e.g., of crystal lattices, crystallites of a polycrystal or grains of a granular material.

Historically, ideas underlying generalized continuum theories were advanced already in the 19th century by Cauchy (1851) and Voigt (1887), but the subject was generalized and reached maturity only in the 1960s and 1970s with the works of Toupin (1962), Mindlin (1964), Bleustein (1967), Mindlin and Eshel (1968), and Germain (1973).

The Toupin-Mindlin gradient theory had already some successful applications on stress concentration elasticity problems concerning holes and inclusions, during the 1960s and 1970s (see e.g. Cook and Weitsman, 1966; Eshel and Rosenfeld, 1970). More recently, this approach and related extensions for microstructured materials have been employed to analyze various problems involving, among other areas, wave propagation (see e.g. Vardoulakis and Georgiadis, 1997; Georgiadis et al., 2000; Georgiadis et al., 2004), fracture (see e.g. Wei and Hutchinson, 1997; Zhang et al., 1998; Chen et al., 1998; 1999; Shi et al., 2000; Georgiadis, 2003; Grentzelou and Georgiadis, 2005; 2008; Wei, 2006; Karlis et al., 2007; Radi, 2008), and plasticity (see e.g. Fleck et al., 1994; Vardoulakis and Sulem, 1995; Begley and Hutchinson, 1998; Fleck and Hutchinson, 1997; 1998; Gao et al. 1999; Huang et al., 2000; 2004; Hwang et al., 2002; Radi, 2007). In addition, efficient numerical techniques (see e.g. Shu et al., 1999; Amanatidou and Aravas, 2002; Tsepoura et al., 2002; Tsamasphyros et al., 2007) have been developed to deal with problems analyzed by the Toupin-Mindlin theory.

Regarding now appropriate length scales for strain gradient theories, as noted by Zhang et al. (1998), although strain gradient effects are associated with geometrically necessary dislocations in plasticity, they may also be important for the *elastic* range in microstructured materials. Indeed, Chen et al. (1998) developed a continuum model for cellular materials and found out that the continuum description of these materials obeys a gradient elasticity theory. In the latter study, the intrinsic material length was naturally identified with the cell size. Also, in wave propagation dealing with electronic-device applications, surface-wave frequencies on the order of GHz are often used and therefore wavelengths on the micron order appear (see e.g. White, 1970). In such situations, *dispersion phenomena* of Rayleigh waves at high frequencies can only be explained on the basis of a

gradient elasticity theory (Georgiadis et al., 2004). In addition, the latter study provides an estimate for a microstructural parameter (i.e. the so-called gradient coefficient c) employed in some simple material models. This was effected by considering that the material is composed wholly of unit cells having the form of cubes with edges of size $2h$ and comparing the forms of dispersion curves of Rayleigh waves obtained by the Toupin-Mindlin approach with the ones obtained by the atomic-lattice analysis of Gazis et al. (1960). It was found that c is of the order of $(0.1h)^2$. Generally, theories with elastic strain gradient effects are intended to model situations where the intrinsic material lengths are of the order of 0.1 – 10 microns (see e.g. Shi et al., 2000). Since the strengthening effects arising from strain gradients become important when these gradients are large enough, these effects will be significant when the material is deformed in *very small* volumes, such as in the immediate vicinity of crack tips, notches, small holes and inclusions, and micrometer indentations.

In the present study, the most common version of the Toupin-Mindlin theory, i.e. the so-called micro-homogeneous case (see Section 10 in Mindlin, 1964), is employed to deal with the plane-strain problem of a *finite-length* crack. According to this, each material particle has three degrees of freedom (the displacement components) and the micro-density does not differ from the macro-density. Also, among the three forms of that version, we chose form II in Mindlin's theory which assumes a strain-energy density that is a function of the strain tensor and its gradient. The latter case is different from the common case of couple-stress theory, which assumes a strain-energy density that depends upon the strain tensor and the gradient of rotation vector (Mindlin and Tiersten, 1962). Notice also that the couple-stress elasticity and form II of Mindlin's gradient elasticity give results for plane-strain boundary value problems that do *not* share the same general features of solution behavior, e.g. order of singularities and crack-face displacements in crack problems (Grentzelou and Georgiadis, 2005). This can be realized from the fact that not only the number of traction boundary conditions are different in the two cases (four in form II of gradient theory, three in couple-stress theory) but, also, the governing equations are different. Therefore, we do not intend to discuss here crack problems within the context of the couple-stress theory but refer the interested reader to the papers by Huang et al. (1997; 1999), and Gourgiotis and Georgiadis (2007; 2008).

Now, we concentrate on the subject of the present work, i.e. *plane-strain* crack problems within the form II of gradient elasticity. In the literature, there are two general results and a few analytical and numerical results related to this subject.

The first general result is a uniqueness theorem for crack problems (Grentzelou and Georgiadis, 2005) showing that a necessary condition for uniqueness within the form II of gradient elasticity, in the absence of body forces, is a bounded strain field around the crack tip in addition to the condition of a bounded displacement field (the latter kinematical condition is the only one that should hold within the classical elasticity – cf. Knowles and Pucik, 1973). The second general result concerns the derivation of the J, L and M integrals for cracks within the gradient elasticity (Georgiadis and Grentzelou, 2006; Grentzelou and Georgiadis, 2008). It was shown that (i) the J-integral (identified with the energy release rate at the crack tip) is path-independent in the case of a quasi-static response and a homogeneous material, (ii) the L-integral is path-independent in the case of a quasi-static response and a homogeneous and isotropic material, and (iii) the M-integral is always path-dependent. The latter result for the M-integral is, of course, in contrast to what happens in classical elasticity – the path-dependence in gradient elasticity is due to the existence of characteristic material lengths that renders the strain-energy density non-invariant under a self-similar scale change. In the present work, after obtaining the stress and displacement fields, we will calculate the J-integral based on the result mentioned before (Georgiadis and Grentzelou, 2006; Grentzelou and Georgiadis, 2008) and reach to important conclusions about the effects of microstructure.

Regarding now solutions of problems closely related to our problem, Shi et al. (2000) studied the elastic problem of a *semi-infinite* crack in a body of infinite extent by considering a gradient theory, which is the limit of a gradient plasticity theory (Fleck and Hutchinson, 1997) with the plastic work hardening exponent $n=1$. A remote classical K field was imposed in this problem. Notice that we treat here the case of a finite-length crack. Moreover, Shi et al. (2000) considered only the case of an incompressible material. This assumption reduced the number of independent boundary conditions along the crack faces, in the plane-strain case, from four to three (two monopolar force tractions and one dipolar force traction). Another work employing the previous framework but without resorting to the incompressibility assumption is due to Wei (2006). This is a numerical study employing finite elements. Finally, Karlis et al. (2007) used the same version of gradient elasticity considered here in a numerical study employing boundary elements. They restricted attention to calculate stress intensities and crack-face displacements. They did not consider asymptotics neither provide calculations of the stress distribution ahead of the crack tip and the energy release rate. Notice that in the present study, besides addressing the latter issues (which are important for the physics of the problem), we also examine the effect of Poisson's ratio in the solution and the ratio of

the crack length over the material length. At any rate, of course, a study based mainly on analytical considerations and providing a detailed full-field solution (like the present one) has an advantage over numerical solutions based on finite or boundary elements, especially in new areas of research where benchmark solutions do not exist.

Our analysis starts with asymptotic considerations for both mode I and II cases. The stress and displacement fields at the vicinity of the crack tip are derived using the Knein-Williams technique. Next, we formulate integral equations, with the aid of Fourier transforms, for the full-field solutions of the boundary value problems. In both mode I and II cases, systems of coupled hypersingular integral equations with a cubic singularity result. Then, these systems of equations are discretized using the collocation method. The numerical solution of the systems shows, in general, that: (i) A cracked solid governed by form II of dipolar gradient elasticity behaves in a more rigid way (having increased stiffness) as compared to a solid governed by classical elasticity. Indeed, the crack-face displacements exhibit an $r^{3/2}$ variation (cusp-like closure), where r is the radial distance from the crack tip. The strain field is also bounded at the crack-tip vicinity and this concurs with the uniqueness theorem mentioned before. (ii) The so-called *total stress* exhibits a typical boundary-layer behavior with an initial very small area, adjacent to the crack tip, of cohesive tractions (with an $r^{-3/2}$ singularity), the tractions then taking on positive values and reaching a bounded maximum. This behavior was also observed before by Shi et al. (2000), Georgiadis (2003), and Wei (2006). Notice that the length of the cohesive-traction area ranges from $0.45c^{1/2}$ to $0.77c^{1/2}$, i.e. this length is very small since c is of the order of $(0.1h)^2$, where $2h$ is the size of the unit cell. (iii) Despite the hypersingular character of stress, it turns out that the J-integral (energy release rate) remains bounded. This is because the crack faces close in a smooth manner. The J-integral in gradient elasticity tends continuously to its counterpart in classical elasticity as $c^{1/2}/a \to 0$, where $c^{1/2}$ is the material length and a is the half of the crack length. For $c^{1/2} \neq 0$, a decrease of its value is noticed in comparison with the classical theory and this indicates that the rigidity effect *dominates* over the stress aggravation effect in the energy release rate. The ratio $J/J^{clas.}$, where $J^{clas.}$ is the expression of the J-integral in classical elastic fracture mechanics, decreases monotonically with increasing values of $c^{1/2}/a$. This finding shows that the gradient theory predicts a strengthening effect since a reduction of the crack driving force ('stress concentration') takes place as the material microstructure becomes more pronounced. An analogous result for stress concentration around cylindrical holes was

observed in an early paper using form II of gradient elasticity where the stress concentration factor decreases for increasing values of material lengths (Eshel and Rosenfeld, 1970).

2. Fundamentals of dipolar gradient elasticity

In this Section, we will give a brief account of form II of Mindlin's theory of dipolar gradient elasticity. More detailed presentations can be found in Mindlin (1964) and in Mindlin and Eshel (1968). The theory is best introduced by the following form of the first law of thermodynamics

$$\rho \dot{\mathsf{E}} = \tau_{pq}\dot{\varepsilon}_{pq} + m_{rpq}\partial_r \dot{\varepsilon}_{pq} \quad , \tag{1}$$

where small strains and displacements are assumed, and a Cartesian rectangular coordinate system $Ox_1x_2x_3$ is considered for a 3D continuum (indicial notation and the summation convention will be used throughout). In the above equation, $\partial_p(\ ) \equiv \partial(\ )/\partial x_p$, a superposed dot denotes time derivative, the Latin indices span the range (1,2,3), ρ is the mass density of the continuum, E is the internal energy per unit mass, $\varepsilon_{pq} = (1/2)(\partial_p u_q + \partial_q u_p) = \varepsilon_{qp}$ is the linear strain tensor, u_q is the displacement vector, τ_{pq} is the monopolar stress tensor, and m_{rpq} is the dipolar (or double) stress tensor (a third-rank tensor) expressed in dimensions of [force][length]$^{-1}$. The nature of the dipolar stresses and the notation used are explained by Mindlin (1964).

Next, in accord with (1), the following form is taken for the strain-energy density W

$$W \equiv W(\varepsilon_{pq}, \partial_r \varepsilon_{pq}) \quad , \tag{2}$$

which is assumed to be a positive definite function. Further, stresses can be defined in the standard variational manner

$$\tau_{pq} \equiv \frac{\partial W}{\partial \varepsilon_{pq}} \quad , \qquad m_{rpq} \equiv \frac{\partial W}{\partial(\partial_r \varepsilon_{pq})} \quad . \tag{3a,b}$$

Then, the equations of equilibrium (global equilibrium) and the *traction* boundary conditions along a smooth boundary (local equilibrium) can be obtained from variational considerations (Mindlin 1964; Bleustein, 1967). Assuming the absence of body forces, the appropriate expression of the Principle of Virtual Work is written as (Bleustein, 1967)

$$\int_V \left[\tau_{pq}\delta\varepsilon_{pq} + m_{rpq}\delta\left(\partial_r\varepsilon_{pq}\right)\right]dV = \int_S t_q^{(n)}\,\delta u_q\,dS + \int_S T_{qr}^{(n)}\,\partial_q\left(\delta u_r\right)dS \quad , \tag{4}$$

where V is the region occupied by the body, and S is the surface of the body. The symbol δ denotes weak variations and it acts on the quantity existing on its right. In the above equation, $t_q^{(n)}$ is the *true* monopolar traction, $T_{pq}^{(n)}$ is the *true* dipolar traction, and n_p is the outward unit normal to the boundary along a section inside the body or along the surface of it. Examples of the dipolar tractions $T_{pq}^{(n)}$ can be found in the work by Georgiadis and Anagnostou (2008).

The equations of equilibrium and the traction boundary conditions take the following form

$$\partial_p\left(\tau_{pq} - \partial_r m_{rpq}\right) = 0 \quad \text{in } V \quad , \tag{5}$$

$$P_q^{(n)} = n_p\left(\tau_{pq} - \partial_r m_{rpq}\right) - D_p\left(n_r m_{rpq}\right) + \left(D_j n_j\right)n_r n_p m_{rpq} \quad \text{on } bdy \quad , \tag{6}$$

$$R_q^{(n)} = n_r n_p m_{rpq} \quad \text{on } bdy \quad , \tag{7}$$

where *bdy* denotes any boundary along a section inside the body or along the surface of it, $D_p(\,) \equiv \partial_p(\,) - n_p D(\,)$ is the surface gradient operator, $D(\,) \equiv n_r\partial_r(\,)$ is the normal gradient operator, $P_q^{(n)} \equiv t_q^{(n)} + \left(D_r n_r\right)n_p T_{pq}^{(n)} - D_p T_{pq}^{(n)}$ is the auxiliary force traction, and $R_q^{(n)} \equiv n_p T_{pq}^{(n)}$ is the auxiliary double force traction. Finally, let S_σ be the portion of the surface S of the body on which external tractions are prescribed.

The kinematical boundary conditions are stated next. These boundary conditions were extracted in the context of the Principle of Complementary Virtual Work (Georgiadis and Grentzelou, 2006):

$$u_q : \text{given on } S_u \quad , \tag{8a}$$

$D(u_q)$: given on S_u , (8b)

where S_u is the portion of the surface S of the body on which both displacements and their normal derivatives are prescribed. Of course, $S_\sigma \cup S_u = S$ and $S_\sigma \cap S_u = \varnothing$ hold true.

Introducing the constitutive equations of the theory is now in order. The simplest possible linear and isotropic equations result from the following strain-energy density function (Georgiadis et al., 2004; Lazar and Maugin, 2005)

$$W = (1/2)\lambda\varepsilon_{pp}\varepsilon_{qq} + \mu\varepsilon_{pq}\varepsilon_{pq} + c(1/2)\lambda(\partial_r\varepsilon_{pp})(\partial_r\varepsilon_{qq}) + c\mu(\partial_r\varepsilon_{pq})(\partial_r\varepsilon_{pq}) \ , \tag{9}$$

where c is the gradient coefficient having dimensions of [length]^2, and (λ, μ) are the standard Lamé constants with dimensions of [force][length]$^{-2}$. In this way, only one new material constant is introduced with respect to classical linear isotropic elasticity. Combining (3) with (9) provides the constitutive equations

$$\tau_{pq} = \lambda\delta_{pq}\varepsilon_{jj} + 2\mu\varepsilon_{pq} \ , \qquad m_{rpq} = c\partial_r(\lambda\delta_{pq}\varepsilon_{jj} + 2\mu\varepsilon_{pq}) \ , \tag{10a,b}$$

where δ_{pq} is the Kronecker delta. Equations (9) and (10) written for a general 3D state will be employed below only for a plane-strain state. As Lazar and Maugin (2005) pointed out, the particular choice of (9) is physically justified and possesses a symmetry of the strain-energy density of the form $W = (1/2)\tau_{pq}\varepsilon_{pq} + c(1/2)(\partial_r\tau_{pq})(\partial_r\varepsilon_{pq})$ showing that this simple constitutive model exhibits dependence upon the *strain* and *stress* gradients.

Notice that fully anisotropic constitutive relations have been used in deriving general results (energy theorems, uniqueness, balance laws and energy release rates) in recent works on gradient elasticity (Grentzelou and Georgiadis, 2005; 2008; Georgiadis and Grentzelou, 2006), but use of the general relations poses serious difficulties in solving specific boundary value problems. Therefore, the assumption of isotropy and the simplification using a *single* material length mentioned above greatly facilitate the analysis of boundary value problems of gradient elasticity. The full constitutive relations in the isotropic case involve five material constants besides the two Lamé constants (Mindlin, 1964).

In summary, (5), (6), (7), (8) and (10) are the governing equations for the isotropic linear gradient elasticity. Combining (5) with (10) leads to the system of field equations. It is noticed that *uniqueness* theorems have been proved on the basis of positive definiteness of the strain-energy density in cases of both regular and singular fields in the recent works of Georgiadis and Grentzelou (2006), and Grentzelou and Georgiadis (2005). Finally, as shown by Georgiadis et al. (2004), the restriction of positive definiteness of W requires the following inequalities for the material constants appearing in the theory employed here $\left(3\lambda+2\mu\right)>0$, $\mu>0$, $c>0$. In addition, *stability* for the field equations in the general inertial case was proved and to accomplish this, the condition $c>0$ is a necessary one.

3. Basic equations in plane strain

We present here the basic equations for a plane-strain state. A body occupying a domain in the (x, y)-plane is considered with the z-axis being normal to this plane. Cartesian coordinates are considered with orthonormal base vectors $\left(\mathbf{e}_x, \mathbf{e}_y\right)$ in the plane considered. All tractions are assumed to act 'inside' the plane (x, y) and are independent upon z. The following 2D displacement field is generated: $u_x \equiv u_x(x, y) \neq 0$, $u_y \equiv u_y(x, y) \neq 0$, $u_z \equiv 0$.

In the plane-strain state, the independent components of the stress tensors that act 'inside' the plane (x, y) and that do not vanish identically are three for τ_{pq} and six for m_{rpq}. Equations (10) are utilized. The components of stresses in Cartesian coordinates are

$$\tau_{xx} = (\lambda + 2\mu)\partial_x u_x + \lambda\partial_y u_y \quad , \quad \tau_{yy} = (\lambda + 2\mu)\partial_y u_y + \lambda\partial_x u_x \quad ,$$
$$\tau_{xy} = \mu(\partial_y u_x + \partial_x u_y) \quad , \tag{11a-c}$$

$$m_{xxx} = c\frac{\partial}{\partial x}\left[(\lambda + 2\mu)\partial_x u_x + \lambda\,\partial_y u_y\right] \quad , \qquad m_{xxy} = c\mu\frac{\partial}{\partial x}(\partial_y u_x + \partial_x u_y) \quad ,$$
$$m_{xyy} = c\frac{\partial}{\partial x}\left[(\lambda + 2\mu)\partial_y u_y + \lambda\,\partial_x u_x\right] \quad , \qquad m_{yxx} = c\frac{\partial}{\partial y}\left[(\lambda + 2\mu)\partial_x u_x + \lambda\,\partial_y u_y\right] \quad ,$$
$$m_{yyy} = c\frac{\partial}{\partial y}\left[(\lambda + 2\mu)\partial_y u_y + \lambda\,\partial_x u_x\right] \quad , \qquad m_{yxy} = c\mu\frac{\partial}{\partial y}(\partial_y u_x + \partial_x u_y) \quad , \tag{12a-f}$$

where $\partial_x(\ ) \equiv \partial(\ )/\partial x$ and $\partial_y(\ ) \equiv \partial(\ )/\partial y$.

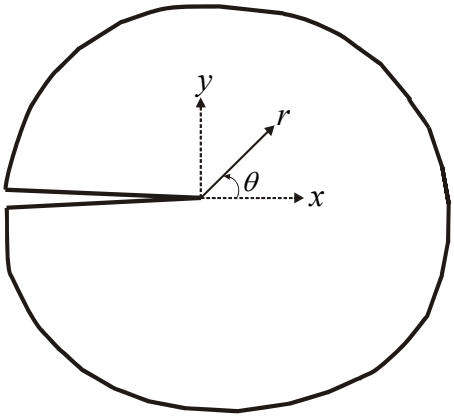

Fig. 1 Cartesian and polar coordinate systems with an origin at the crack tip.

In our asymptotic analysis, we will need to employ polar coordinates (r,θ) with orthonormal base vectors $(\mathbf{e}_r,\mathbf{e}_\theta)$. The system of these coordinates is shown in Fig. 1 and the stresses are now written as

$$\tau_{rr} = (\lambda+2\mu)\,\partial_r u_r + \lambda\, r^{-1}(u_r + \partial_\theta u_\theta)\ , \quad \tau_{\theta\theta} = (\lambda+2\mu) r^{-1}(u_r + \partial_\theta u_\theta) + \lambda \partial_r u_r\ ,$$
$$\tau_{r\theta} = \mu[r^{-1}(\partial_\theta u_r - u_\theta) + \partial_r u_\theta]\ , \tag{13a-c}$$

$$m_{rrr} = c\partial_r \tau_{rr}\ , \quad m_{rr\theta} = c\partial_r \tau_{r\theta}\ , \quad m_{r\theta\theta} = c\partial_r \tau_{\theta\theta}\ , \quad m_{\theta rr} = cr^{-1}(\partial_\theta \tau_{rr} - 2\tau_{r\theta})\ ,$$
$$m_{\theta\theta r} = cr^{-1}(\partial_\theta \tau_{\theta r} + \tau_{rr} - \tau_{\theta\theta})\ , \quad m_{\theta\theta\theta} = cr^{-1}(\partial_\theta \tau_{\theta\theta} + 2\tau_{r\theta})\ , \tag{14a-f}$$

where $\partial_r(\ ) \equiv \partial(\ )/\partial r$ and $\partial_\theta(\ ) \equiv \partial(\ )/\partial\theta$.

Next, we introduce the *total stresses*. These quantities result from the monopolar traction conditions (Georgiadis 2003; Georgiadis and Grentzelou, 2006). To define the total stresses arisen in our boundary value problems in Cartesian coordinates, we consider a plane $(x, y = \text{const.})$. The normal unit vector to this plane is given as $\mathbf{n} = (0, \pm 1)$. Then, the total stresses *along this plane* are defined as

$$t_{yx} \equiv P_x^{(n)} = \tau_{yx} - \frac{\partial m_{xyx}}{\partial x} - \frac{\partial m_{yyx}}{\partial y} - \frac{\partial m_{yxx}}{\partial x} \ , \tag{15}$$

$$t_{yy} \equiv P_y^{(n)} = \tau_{yy} - \frac{\partial m_{xyy}}{\partial x} - \frac{\partial m_{yyy}}{\partial y} - \frac{\partial m_{yxy}}{\partial x} \ . \tag{16}$$

In polar coordinates, we consider a plane $(r, \theta = \text{const.})$ and define the total stresses along this plane as

$$t_{\theta r} \equiv P_r^{(n)} = \tau_{\theta r} - \frac{\partial m_{\theta rr}}{\partial r} - \frac{\partial m_{r\theta r}}{\partial r} - \frac{1}{r}\frac{\partial m_{\theta\theta r}}{\partial \theta} - \frac{1}{r} m_{\theta rr} - \frac{1}{r} m_{r\theta r} + \frac{1}{r} m_{\theta\theta\theta} \ , \tag{17}$$

$$t_{\theta\theta} \equiv P_\theta^{(n)} = \tau_{\theta\theta} - \frac{\partial m_{\theta r\theta}}{\partial r} - \frac{\partial m_{r\theta\theta}}{\partial r} - \frac{1}{r}\frac{\partial m_{\theta\theta\theta}}{\partial \theta} - \frac{1}{r} m_{r\theta\theta} - \frac{2}{r} m_{\theta r\theta} \ . \tag{18}$$

It is noted that the total stress along the crack plane and ahead of the crack tip enters the expression for the energy release rate. Moreover, the normal total stress ahead of the crack tip can be related with the cleavage strength of the material. The derivation of (17) and (18) is given in Appendix A.

Finally, substituting the constitutive relations (11) and (12) in the equations of equilibrium (Eqs. (5)) leads to the following system of coupled PDEs of the fourth order for the displacement components

$$(1 - c\nabla^2)[2(1-\nu)\partial_x(\partial_x u_x + \partial_y u_y) - (1-2\nu)\,\partial_y(\partial_x u_y - \partial_y u_x)] = 0 \ , \tag{19a}$$

$$(1 - c\nabla^2)[2(1-\nu)\partial_y(\partial_x u_x + \partial_y u_y) + (1-2\nu)\,\partial_x(\partial_x u_y - \partial_y u_x)] = 0 \ , \tag{19b}$$

in Cartesian coordinates, and

$$s_r - c[\nabla^2 s_r - r^{-2} s_r - 2r^{-2}\partial_\theta s_\theta] = 0 \ , \tag{20a}$$

$$s_\theta - c[\nabla^2 s_\theta - r^{-2} s_\theta + 2r^{-2}\partial_\theta s_r] = 0 \ , \tag{20b}$$

in polar coordinates. In the above equations, $\nu = \lambda/2(\lambda+\mu)$ is the Poisson's ratio, $\nabla^2(\,) \equiv$ $\equiv \partial_x^2(\,) + \partial_y^2(\,) \equiv \partial_r^2(\,) + r^{-1}\partial_r(\,) + r^{-2}\partial_\theta^2(\,)$ is the 2D Laplace operator, and the quantities (s_r, s_θ) are given as

$$s_r = 2(1-\nu)\partial_r(\partial_r u_r + r^{-1}\partial_\theta u_\theta + r^{-1}u_r) - (1-2\nu)r^{-1}\partial_\theta(\partial_r u_\theta - r^{-1}\partial_\theta u_r + r^{-1}u_\theta) \ , \tag{21a}$$

$$s_\theta = 2(1-\nu)r^{-1}\partial_\theta(\partial_r u_r + r^{-1}\partial_\theta u_\theta + r^{-1}u_r) + (1-2\nu)\partial_r(\partial_r u_\theta - r^{-1}\partial_\theta u_r + r^{-1}u_\theta) \ . \tag{21b}$$

The details of the derivation of (20) are given in Appendix A. Finally, in the limit $c \to 0$, the Navier-Cauchy equations of classical linear isotropic elasticity are recovered from (19) or (20).

4. Asymptotic fields around the crack tip

In this Section, the Knein-Williams asymptotic technique (Knein, 1927; Williams, 1952; Barber, 1992) is employed to explore the nature of the stress and displacement fields near the crack tip. This is accomplished by attaching a set of (r,θ) polar coordinates at the crack tip and by expanding the displacement field as an asymptotic series of separated variable terms, each satisfying the traction-free boundary conditions on the crack faces defined by $\mathbf{n} = \pm\mathbf{e}_\theta$ (see Fig. 1). Thus, the leading terms of the displacement components are written as

$$u_r(r,\theta) = r^p\, U_r(\theta) \ , \quad u_\theta(r,\theta) = r^p\, U_\theta(\theta) \ , \tag{22}$$

where p is a complex (in general) constant to be determined.

The boundary conditions for a traction-free crack at $\theta = \pm\pi$ read

$$t_{\theta\theta}(r,\pm\pi) = 0 \ , \quad t_{\theta r}(r,\pm\pi) = 0 \ , \quad m_{\theta\theta r}(r,\pm\pi) = 0 \ , \quad m_{\theta\theta\theta}(r,\pm\pi) = 0 \ . \tag{23}$$

Further, if only the dominant singular terms are retained in the asymptotic fields, the governing equations in (20) become

$$\nabla^2 s_r - r^{-2} s_r - 2r^{-2}\partial_\theta s_\theta = 0 \ , \tag{24a}$$

$$\nabla^2 s_\theta - r^{-2} s_\theta + 2r^{-2}\partial_\theta s_r = 0 \ . \tag{24b}$$

A general solution to (24) is obtained as

$$\begin{aligned} u_r &= r^p\left[A_1\cos((p-1)\theta) + A_2\cos((p+1)\theta) + A_3\cos((p-3)\theta)\right] \\ &\quad + r^p\left[B_1\sin((p-1)\theta) + B_2\sin((p+1)\theta) + B_3\sin((p-3)\theta)\right] , \end{aligned} \tag{25a}$$

$$\begin{aligned} u_\theta &= r^p\left[A_4\sin((p-1)\theta) - A_2\sin((p+1)\theta) - A_3\frac{(p+5-8\nu)}{(p-7+8\nu)}\sin((p-3)\theta)\right] \\ &\quad + r^p\left[B_4\cos((p-1)\theta) + B_2\cos((p+1)\theta) + B_3\frac{(p+5-8\nu)}{(p-7+8\nu)}\cos((p-3)\theta)\right] , \end{aligned} \tag{25b}$$

where A_b and B_b (with $b = 1,2,3,4$) are unknown constants, corresponding to mode I and mode II cases, respectively.

Next, we utilize the constitutive equations in (13) and (14), retain only the most singular terms and write the boundary conditions in terms of displacements at $\theta = \pm\pi$

$$\begin{aligned} t_{\theta r}(r,\pm\pi) = 0 \ &\Rightarrow \ -\partial_r m_{\theta rr} - \partial_r m_{r\theta r} - r^{-1}\partial_\theta m_{\theta\theta r} - r^{-1} m_{\theta rr} - r^{-1} m_{r\theta r} + r^{-1} m_{\theta\theta\theta} = 0 \ \Rightarrow , \\ &\Rightarrow \ -(3-4\nu) r^2\,\partial_r^2\partial_\theta u_r + (3-2\nu)\partial_\theta u_r + (5-6\nu)\partial_\theta^2 u_\theta - r\,\partial_\theta^2\partial_r u_\theta \\ &\quad + (1-2\nu)\left[-r^3\partial_r^3 u_\theta + 2r^2\,\partial_r^2 u_\theta + r\partial_r\partial_\theta u_r - r\partial_r u_\theta - \partial_\theta^3 u_r + u_\theta\right] = 0 \ , \end{aligned} \tag{26}$$

$$\begin{aligned} t_{\theta\theta}(r,\pm\pi) = 0 \ &\Rightarrow \ -\partial_r m_{\theta\theta r} - \partial_r m_{r\theta\theta} - r^{-1}\partial_\theta m_{\theta\theta\theta} - r^{-1} m_{r\theta\theta} - 2r^{-1} m_{\theta\theta r} = 0 \ \Rightarrow , \\ &\Rightarrow \ (3-4\nu) r^2\,\partial_r^2\partial_\theta u_\theta + 2(2-3\nu)\partial_\theta^2 u_r + 2\nu\, r^3\partial_r^3 u_r + 2\nu\,\partial_\theta u_\theta + r\,\partial_\theta^2\partial_r u_r \\ &\quad + (1-\nu)\left[4r^2\partial_r^2 u_r + 2\partial_\theta^3 u_\theta - 2r\partial_r\partial_\theta u_\theta - 2r\partial_r u_r + 2u_r\right] = 0 \ , \end{aligned} \tag{27}$$

$$m_{\theta\theta r}(r,\pm\pi) = 0 \ \Rightarrow \ \partial_r\left(r^{-1}(2u_r + \partial_\theta u_\theta)\right) + r^{-2}\partial_\theta(\partial_\theta u_r - 2u_\theta) = 0 \ , \tag{28}$$

$$m_{\theta\theta\theta}(r,\pm\pi) = 0 \ \Rightarrow \ (1-\nu)\left(\partial_r(r^{-1}u_\theta) + r^{-2}\partial_\theta(2u_r + \partial_\theta u_\theta)\right) + \nu\,\partial_r\left(r^{-1}(\partial_\theta u_r - u_\theta)\right) = 0 \ . \tag{29}$$

Now, (26)-(29) together with (25) constitute an *eigenvalue* problem. For the existence of a non-trivial solution, the determinant of the coefficients of (A_b, B_b) should vanish and this gives, for both plane-strain modes, the following equation for p

$$(p-1)^4(p-2)^2[1-\cos(4\pi p)]=0 \quad \Rightarrow \quad p=\frac{n}{2}, \quad n=0,1,2,... \quad . \tag{30}$$

The appropriate eigenvalue will be determined from the requirement of a bounded strain energy in the vicinity of the crack tip. The detailed procedure within classical elasticity is described by Barber (1992). By noticing that in our case the strain-energy density behaves at most as $W \approx \left(\partial_r \varepsilon_{ij}\right)^2$, we conclude that the integrability of W requires that the following inequality be satisfied $2(p-2)+1>-1 \Rightarrow p>1$. Thus, the *most singular* admissible value of the exponent is $p=3/2$. However, it is noted that the eigenvalue $p=1$ also satisfies (30). In this case, a *constant* strain field results which does not contribute to dipolar stresses (this is because $\nabla\boldsymbol{\varepsilon}=0$, in this case). In this special case, the strain-energy density W in (9) behaves as in classical elasticity, i.e. $W \approx \varepsilon_{pq}^2$ and it is bounded. As will be shown below, this constant (lowest-order) term, which is analogous to the T-stress field in classical fracture mechanics (see e.g. Anderson, 1995), does *not* contribute to the J-integral and to the crack opening displacement. We also notice that the existence of a field associated with the eigenvalue $p=1$ was first pointed out by Radi (2008) for the mode III crack problem in couple-stress elasticity. Aravas and Giannakopoulos (2009) made a similar observation in strain gradient elasticity. Finally, we note that the case $p<1$ is excluded since it *always* leads to unbounded strain energy in the vicinity of the crack tip.

Below, the cases of mode I and II asymptotic crack-tip fields for $r \to 0$ will be presented separately.

4.1 Mode I asymptotic crack-tip field

In view of the symmetry of the mode I problem, we obtain the corresponding displacement field as

$$u_r = r\left[\Gamma_1 + \Gamma_2 \cos 2\theta\right] + A_1 r^{3/2}\left[(3-8\nu)\cos\frac{\theta}{2} + 3\frac{(11-16\nu)}{(41-32\nu)}\cos\frac{3\theta}{2}\right]$$
$$- A_2 r^{3/2}\left[3\frac{(11-16\nu)}{(41-32\nu)}\cos\frac{3\theta}{2} - \cos\frac{5\theta}{2}\right], \tag{31a}$$

$$u_\theta = -\Gamma_2 r \sin 2\theta + A_1 r^{3/2}\left[(9-8\nu)\sin\frac{\theta}{2} - 3\frac{(13-16\nu)}{(41-32\nu)}\sin\frac{3\theta}{2}\right]$$
$$+ A_2 r^{3/2}\left[3\frac{(13-16\nu)}{(41-32\nu)}\sin\frac{3\theta}{2} - \sin\frac{5\theta}{2}\right], \tag{31b}$$

where (Γ_1, Γ_2) are the amplitude factors for the lowest-order crack-tip fields and (A_1, A_2) are the amplitude factors for the dominant terms of order $3/2$. All these constants are left unspecified by the asymptotic analysis. One may observe that along the crack faces $(\theta = \pm\pi)$ the term $-\Gamma_2 r \sin 2\theta$ vanishes and, therefore, the lowest-order does not contribute to the crack opening displacement.

In addition, by virtue of (13), (14) and appropriate definitions in the previous analysis, the monopolar, dipolar and total stresses are written as

$$\tau_{rr} = \left[2\mu\Gamma_1/(1-2\nu)\right] + 2\mu\Gamma_2\cos 2\theta + 3\mu A_1 r^{1/2}\left[3\cos\frac{\theta}{2} + \frac{(33-32\nu)}{41-32\nu}\cos\frac{3\theta}{2}\right]$$
$$- 3\mu A_2 r^{1/2}\left[\frac{(33-32\nu)}{41-32\nu}\cos\frac{3\theta}{2} - \cos\frac{5\theta}{2}\right]. \tag{32a}$$

$$\tau_{\theta\theta} = \left[2\mu\Gamma_1/(1-2\nu)\right] - 2\mu\Gamma_2\cos 2\theta + 3\mu A_1 r^{1/2}\left[5\cos\frac{\theta}{2} - \frac{(17-32\nu)}{41-32\nu}\cos\frac{3\theta}{2}\right]$$
$$- 3\mu A_2 r^{1/2}\left[-\frac{(17-32\nu)}{41-32\nu}\cos\frac{3\theta}{2} + \cos\frac{5\theta}{2}\right], \tag{32b}$$

$$\tau_{\theta r} = \tau_{r\theta} = -2\mu\Gamma_2\sin 2\theta + 3\mu A_1 r^{1/2}\left[\sin\frac{\theta}{2} - \frac{(23-32\nu)}{41-32\nu}\sin\frac{3\theta}{2}\right]$$
$$- 3\mu A_2 r^{1/2}\left[-\frac{(23-32\nu)}{41-32\nu}\sin\frac{3\theta}{2} + \sin\frac{5\theta}{2}\right], \tag{32c}$$

$$m_{\theta\theta r} = \frac{3\mu c}{2} A_1 r^{-1/2}\left[-3\cos\frac{\theta}{2} + \frac{(31-32\nu)}{41-32\nu}\cos\frac{3\theta}{2}\right]$$
$$- \frac{3\mu c}{2} A_2 r^{-1/2}\left[\frac{(31-32\nu)}{41-32\nu}\cos\frac{3\theta}{2} + \cos\frac{5\theta}{2}\right], \tag{33a}$$

$$m_{\theta\theta\theta} = -\frac{3\mu c}{2} A_1 r^{-1/2}\left[\sin\frac{\theta}{2} + \sin\frac{3\theta}{2}\right] + \frac{3\mu c}{2} A_2 r^{-1/2}\left[\sin\frac{3\theta}{2} + \sin\frac{5\theta}{2}\right], \tag{33b}$$

$$m_{rrr} = \frac{3\mu c}{2} A_1 r^{-1/2}\left[3\cos\frac{\theta}{2} + \frac{(33-32\nu)}{41-32\nu}\cos\frac{3\theta}{2}\right]$$

$$-\frac{3\mu c}{2} A_2 r^{-1/2}\left[\frac{(33-32\nu)}{41-32\nu}\cos\frac{3\theta}{2} - \cos\frac{5\theta}{2}\right], \tag{33c}$$

$$m_{r\theta r} = \frac{3\mu c}{2} A_1 r^{-1/2}\left[\sin\frac{\theta}{2} - \frac{(23-32\nu)}{41-32\nu}\sin\frac{3\theta}{2}\right]$$

$$+\frac{3\mu c}{2} A_2 r^{-1/2}\left[\frac{(23-32\nu)}{41-32\nu}\sin\frac{3\theta}{2} - \sin\frac{5\theta}{2}\right], \tag{33d}$$

$$m_{\theta rr} = -\frac{3\mu c}{2} A_1 r^{-1/2}\left[7\sin\frac{\theta}{2} + \frac{(7+32\nu)}{41-32\nu}\sin\frac{3\theta}{2}\right]$$

$$+\frac{3\mu c}{2} A_2 r^{-1/2}\left[\frac{(7+32\nu)}{41-32\nu}\sin\frac{3\theta}{2} - \sin\frac{5\theta}{2}\right], \tag{33e}$$

$$m_{r\theta\theta} = \frac{3\mu c}{2} A_1 r^{-1/2}\left[5\cos\frac{\theta}{2} - \frac{(17-32\nu)}{41-32\nu}\cos\frac{3\theta}{2}\right]$$

$$+\frac{3\mu c}{2} A_2 r^{-1/2}\left[\frac{(17-32\nu)}{41-32\nu}\cos\frac{3\theta}{2} - \cos\frac{5\theta}{2}\right], \tag{33f}$$

$$t_{\theta r} = \frac{3\mu c}{4} A_1 r^{-3/2}\left[\sin\frac{\theta}{2} + \sin\frac{3\theta}{2}\right] - \frac{3\mu c}{4} A_2 r^{-3/2}\left[\sin\frac{3\theta}{2} + \sin\frac{5\theta}{2}\right], \tag{34a}$$

$$t_{\theta\theta} = \frac{3\mu c}{4} A_1 r^{-3/2}\left[\frac{(47-32\nu)}{41-32\nu}\cos\frac{3\theta}{2} + 5\cos\frac{\theta}{2}\right]$$

$$-\frac{3\mu c}{4} A_2 r^{-3/2}\left[\frac{(47-32\nu)}{41-32\nu}\cos\frac{3\theta}{2} + \cos\frac{5\theta}{2}\right]. \tag{34b}$$

4.2 Mode II asymptotic crack-tip field

In view of the antisymmetry of the mode II problem, we obtain the corresponding displacement field as

$$u_r = \Gamma_3\, r \sin 2\theta + B_1\, r^{3/2} \sin\frac{\theta}{2} + B_2\, r^{3/2}\left[-\frac{3(11-16\nu)}{37-32\nu}\sin\frac{3\theta}{2} + \sin\frac{5\theta}{2}\right], \tag{35a}$$

$$u_\theta = \Gamma_3\, r \cos 2\theta - B_1\, r^{3/2} \cos\frac{\theta}{2} + B_2\, r^{3/2}\left[\cos\frac{5\theta}{2} - \frac{3(13-16\nu)}{37-32\nu}\cos\frac{3\theta}{2} + \frac{12}{37-32\nu}\cos\frac{\theta}{2}\right]. \tag{35b}$$

where the constants (Γ_3, B_1, B_2) are amplitude factors left unspecified by the asymptotic analysis.

By virtue of Eqs. (13), (14) and appropriate definitions in the previous analysis, the monopolar, dipolar and total stresses are written in this case as

$$\tau_{rr} = 2\mu\Gamma_3 \sin 2\theta - 3\mu B_2\, r^{1/2}\left[\frac{4\nu}{(1-2\nu)(37-32\nu)}\sin\frac{\theta}{2} + \frac{(33-32\nu)}{37-32\nu}\sin\frac{3\theta}{2} - \sin\frac{5\theta}{2}\right] + \frac{3\mu}{1-2\nu} B_1\, r^{1/2} \sin\frac{\theta}{2}, \tag{36a}$$

$$\tau_{\theta\theta} = -2\mu\Gamma_3 \sin 2\theta - 3\mu B_2\, r^{1/2}\left[\frac{4(1-\nu)}{(1-2\nu)(37-32\nu)}\sin\frac{\theta}{2} - \frac{(17-32\nu)}{37-32\nu}\sin\frac{3\theta}{2} + \sin\frac{5\theta}{2}\right] + \frac{3\mu}{1-2\nu} B_1\, r^{1/2} \sin\frac{\theta}{2}, \tag{36b}$$

$$\tau_{\theta r} = \tau_{r\theta} = 2\mu\Gamma_3 \cos 2\theta + 3\mu B_2\, r^{1/2}\left[\frac{2}{37-32\nu}\cos\frac{\theta}{2} - \frac{(23-32\nu)}{37-32\nu}\cos\frac{3\theta}{2} + \cos\frac{5\theta}{2}\right], \tag{36c}$$

$$m_{\theta\theta\theta} = -\frac{3\mu c}{2} B_2\, r^{-1/2}\left[-\frac{4(1-3\nu)}{(1-2\nu)(37-32\nu)}\cos\frac{\theta}{2} + \frac{(41-32\nu)}{37-32\nu}\cos\frac{3\theta}{2} + \cos\frac{5\theta}{2}\right] + \frac{3\mu c}{2(1-2\nu)} B_1\, r^{-1/2} \cos\frac{\theta}{2}, \tag{37a}$$

$$m_{\theta\theta r} = -\frac{3\mu c}{2} B_2\, r^{-1/2}\left[-\frac{6}{37-32\nu}\sin\frac{\theta}{2} + \frac{(31-32\nu)}{37-32\nu}\sin\frac{3\theta}{2} + \sin\frac{5\theta}{2}\right], \tag{37b}$$

$$m_{rrr} = -\frac{3\mu c}{2} B_2\, r^{-1/2}\left[-\sin\frac{5\theta}{2} + \frac{(33-32\nu)}{37-32\nu}\sin\frac{3\theta}{2} + \frac{4\nu}{(37-32\nu)(1-2\nu)}\sin\frac{\theta}{2}\right] + \frac{3\mu c}{2(1-2\nu)} B_1\, r^{-1/2} \sin\frac{\theta}{2}, \tag{37c}$$

$$m_{\theta rr} = -\frac{3\mu c}{2} B_2\, r^{-1/2}\left[\frac{4(2-3\nu)}{(1-2\nu)(37-32\nu)}\cos\frac{\theta}{2} + \frac{(7+32\nu)}{37-32\nu}\cos\frac{3\theta}{2} - \cos\frac{5\theta}{2}\right]$$

$$+\frac{3\mu c}{2(1-2\nu)}B_1 r^{-1/2}\cos\frac{\theta}{2}\ , \tag{37d}$$

$$m_{r\theta\theta}=-\frac{3\mu c}{2}B_2 r^{-1/2}\left[\frac{4(1-\nu)}{(37-32\nu)(1-2\nu)}\sin\frac{\theta}{2}-\frac{(17-32\nu)}{37-32\nu}\sin\frac{3\theta}{2}+\sin\frac{5\theta}{2}\right]$$

$$+\frac{3\mu c}{2(1-2\nu)}B_1 r^{-1/2}\sin\frac{\theta}{2}\ . \tag{37e}$$

$$m_{r\theta r}=-\frac{3\mu c}{2}B_2 r^{-1/2}\left[-\frac{2}{37-32\nu}\cos\frac{\theta}{2}+\frac{(23-32\nu)}{37-32\nu}\cos\frac{3\theta}{2}-\cos\frac{5\theta}{2}\right]\ , \tag{37f}$$

$$t_{\theta r}=\frac{3\mu c}{4}B_2 r^{-3/2}\left[\frac{4(2-5\nu)}{(1-2\nu)(37-32\nu)}\cos\frac{\theta}{2}+\frac{(41-32\nu)}{37-32\nu}\cos\frac{3\theta}{2}+\cos\frac{5\theta}{2}\right]$$

$$+\frac{3\mu c}{4(1-2\nu)}B_1 r^{-3/2}\cos\frac{\theta}{2}\ , \tag{38a}$$

$$t_{\theta\theta}=-\frac{3\mu c}{4}B_2 r^{-3/2}\left[\frac{10}{37-32\nu}\sin\frac{\theta}{2}+\frac{(47-32\nu)}{37-32\nu}\sin\frac{3\theta}{2}+\sin\frac{5\theta}{2}\right]\ . \tag{38b}$$

In view of all previous asymptotic results, we now notice the following points:

(i) The displacement field in both mode I and II cases is expressed as a sum of a linear in r term (lowest-order term) that gives rise to a constant strain field, and a dominant $r^{3/2}$ term that defines the singular behavior of the dipolar and total stresses. The linear term does not contribute to the crack opening displacement. The crack faces close more smoothly as compared to the classical result exhibiting a variation $\sim r^{3/2}$. This cusp-like closure has been observed in the experiments by Elssner et al. (1994) and in the analyses by Shi et al. (2000) and Cleveringa et al. (2000).

(ii) The strain field is bounded at the crack-tip region. Thus, the necessary condition for uniqueness of the crack problem in form II of Mindlin's gradient elasticity (Grentzelou and Georgiadis, 2005) is fulfilled by the present asymptotic solution.

(iii) The monopolar stresses are bounded in the vicinity of the crack-tip. The constant (independent upon the radial distance r) terms in the asymptotic expansion for the monopolar stresses (see Eqs. (32) and (36)) correspond to the T-stress field of classical fracture mechanics. However, in contrast with what happens in classical elasticity, where the T-stress field appears only in the mode I crack problem (Anderson, 1995), it is observed here that a constant stress field exists in both plane-strain modes. This is justified from the fact that the $O(r)$ terms (in the asymptotic

expansions for the displacements in both mode I and II cases) are coupled, through the boundary conditions (23), with the $O\left(r^{3/2}\right)$ terms.

(iv) The field of total stresses ahead of the crack tip exhibits a stronger singularity ($\sim r^{-3/2}$) than the one predicted by standard linear fracture mechanics. This behavior is in agreement with the analytical results of Shi et al. (2000). Such a strong singularity was also suggested by the experimental evidence of Prakash et al. (1992) in extremely brittle fracture.

5. Integral equation solution

For the full-field analytical solution, we will formulate systems of integral equations. The boundary value problems of mode I and mode II finite-length cracks are attacked initially with the Fourier transform. In classical elasticity, the general procedure of reducing mixed boundary value problems to singular integral equations is given, e.g., by Erdogan (1978). Other more recent applications of this procedure in problems involving a more complex material response (coupled thermoelasticity) were given by Brock and Georgiadis (2000; 2007). Also, an application of the technique within the context of gradient elasticity for anti-plane shear crack problems can be found in Chan et al. (2003). In the present case, systems of *hypersingular* integral equations arise.

Due to the symmetry (antisymmetry) of mode I (mode II) crack problem w.r.t. the plane $y=0$, only the upper half-plane domain ($-\infty < x < \infty,\ y \geq 0$) will be considered. In this domain, the Fourier transform is utilized to suppress the x-dependence in the field equations and the boundary conditions. The direct Fourier transform and its inverse are defined as follows

$$f^*(\xi,y)=\frac{1}{(2\pi)^{1/2}}\int_{-\infty}^{\infty} f(x,y)e^{\mathrm{i}x\xi}dx\ , \tag{39a}$$

$$f(x,y)=\frac{1}{(2\pi)^{1/2}}\int_{-\infty}^{\infty} f^*(\xi,y)e^{-\mathrm{i}x\xi}d\xi\ , \tag{39b}$$

where $\mathrm{i}\equiv(-1)^{1/2}$. Transforming (19) with (39a) gives a system of ODEs for $\left(u_x^*,u_y^*\right)$ written in the following compact form

$$\left[K\right]\begin{bmatrix} u_x^* \\ u_y^* \end{bmatrix} = \begin{bmatrix} 0 \\ 0 \end{bmatrix} \ , \tag{40}$$

where the differential operator $\left[K\right]$ is given as

$$\left[K\right] = \begin{bmatrix} -\left[1+c\left(\xi^2 - d'^2\right)\right]\left[d'^2 + 2(1-\nu)\left(\xi^2 - d'^2\right)\right] & -\mathrm{i}\,\xi d'\left[1+c\left(\xi^2 - d'^2\right)\right] \\ -\mathrm{i}\,\xi d'\left[1+c\left(\xi^2 - d'^2\right)\right] & \left[1+c\left(\xi^2 - d'^2\right)\right]\left[\xi^2 - 2(1-\nu)\left(\xi^2 - d'^2\right)\right] \end{bmatrix} , \tag{41}$$

with $d'(\,) \equiv d(\,)/dy$, $d'^2(\,) \equiv d^2(\,)/dy^2$, etc.

The system of homogeneous differential equations in (40) has a solution different than the trivial one if and only if the determinant of $\left[K\right]$ is zero. Hence,

$$\left(\xi^2 - d'^2\right)^2\left[1+c\left(\xi^2 - d'^2\right)\right]^2 = 0 \ . \tag{42}$$

The above equation has two double roots: $d' = \pm|\xi|$ and $d' = \pm\left[(1/c) + \xi^2\right]^{1/2}$. The first pair is the same as in classical elasticity, whereas the second pair reflects the presence of gradient effects. The general solution of (40) is obtained after some rather extensive algebra and it has the following form for the case of bounded $\left(u_x^*, u_y^*\right)$ as $y \to +\infty$

$$u_x^*(\xi, y) = \mathrm{i}\,\xi^{-1}|\xi| C_1(\xi) e^{-|\xi| y} + \mathrm{i}\,\xi^{-1} C_2(\xi)\left[y|\xi| - (3-4\nu)\right] e^{-|\xi| y} + C_4(\xi) e^{-y\beta} \ , \tag{43a}$$

$$u_y^*(\xi, y) = C_1(\xi) e^{-|\xi| y} + C_2(\xi) y\, e^{-|\xi| y} + C_3(\xi) e^{-y\beta} \ , \tag{43b}$$

where $\beta \equiv \beta(\xi) = \left[(1/c) + \xi^2\right]^{1/2}$. The functions $C_b(\xi)$ (with $b = 1,2,3,4$) are yet unknown functions that will be determined through the enforcement of boundary conditions in each specific problem.

Now, since we have available the transformed general solution in (43), we can enforce the definitions of stresses in Section 3 along with the Fourier-transform inversion in (39b) and write the total and dipolar stresses as

$$t_{yx}=\frac{\mu}{(2\pi)^{1/2}}\int_{-\infty}^{\infty}\Big\{2\mathrm{i}c\beta^2\big[-\xi C_1(\xi)+\big(2(1-\nu)\mathrm{sgn}(\xi)-y\xi\big)C_2(\xi)\big]e^{-y|\xi|}$$
$$+\frac{2c\xi\beta}{(1-2\nu)}\big[\mathrm{i}\nu\beta C_3(\xi)-\xi(1-\nu)C_4(\xi)\big]e^{-y\beta}\Big\}e^{-\mathrm{i}x\xi}d\xi\ , \qquad (44)$$

$$t_{yy}=\frac{\mu}{(2\pi)^{1/2}}\int_{-\infty}^{\infty}\Big\{2c\beta^2\big[-|\xi|C_1(\xi)+\big(1-2\nu-y|\xi|\big)C_2(\xi)\big]e^{-y|\xi|}$$
$$+\xi c\beta\big[\mathrm{i}\beta C_4(\xi)-\xi C_3(\xi)\big]e^{-y\beta}\Big\}e^{-\mathrm{i}x\xi}d\xi\,, \qquad (45)$$

$$m_{yyy}=\frac{\mu}{(2\pi)^{1/2}}\int_{-\infty}^{\infty}\Big\{2c\big[\xi^2C_1(\xi)-\big(2(1-\nu)|\xi|-y\xi^2\big)C_2(\xi)\big]e^{-y|\xi|}$$
$$+\frac{2c\beta}{(1-2\nu)}\big[\beta(1-\nu)C_3(\xi)+\mathrm{i}\nu\xi C_4(\xi)\big]e^{-y\beta}\Big\}e^{-\mathrm{i}x\xi}d\xi\ , \qquad (46)$$

$$m_{yyx}=\frac{\mu}{(2\pi)^{1/2}}\int_{-\infty}^{\infty}\Big\{2\mathrm{i}c\xi\big[|\xi|C_1(\xi)-\big(3-2\nu-y|\xi|\big)C_2(\xi)\big]e^{-y|\xi|}$$
$$+\beta c\big[\mathrm{i}\xi C_3(\xi)+\beta C_4(\xi)\big]e^{-y\beta}\Big\}e^{-\mathrm{i}x\xi}d\xi\ , \qquad (47)$$

where $\mathrm{sgn}(\ )$ is the signum function.

Below, the mode I and mode II cases will be treated separately.

5.1 Mode I crack

Consider a straight crack of length $2a$ in a body of infinite extent. Plane-strain conditions are assumed to prevail, the crack faces are traction free and the body is under a field of pure tension (see Fig. 2). The crack faces are defined by $\mathbf{n}=(0,\pm1)$.

Then, according to (6)-(8), the following mixed boundary conditions hold in the upper half-plane ($y\geq 0$)

$$t_{yy}(x,0)=0\ ,\quad m_{yyx}(x,0)=0 \qquad \text{for}\ \ |x|<a\ , \qquad (48a,b)$$

$$t_{yx}(x,0)=0\ ,\quad m_{yyy}(x,0)=0 \qquad \text{for}\ \ -\infty<x<\infty\ , \qquad (49a,b)$$

$$u_y(x,0)=0\ ,\quad Du_x(x,0)\equiv\partial_y u_x(x,0)=0 \qquad \text{for}\ \ |x|>a\ , \qquad (50a,b)$$

whereas the regularity conditions at infinity are written as

$$t_{yy}^{\infty} \to \sigma_0 \ , \quad t_{xx}^{\infty}, t_{yx}^{\infty}, t_{xy}^{\infty} \to 0 \ , \quad m_{rpq} \to 0 \quad (r,p,q = x,y) \quad \text{as} \quad R \to \infty \ , \tag{51}$$

where $R = \left(x^2 + y^2\right)^{1/2}$ is the distance from the origin and the constant σ_0 denotes the remotely applied normal loading. It is noted that the boundary conditions (49) are valid indeed on the whole crack-line ($-\infty < x < \infty$, $y = 0$). This is due to the fact that the dipolar stress m_{yyy} and the total shear stress t_{yx} are antisymmetric w.r.t. the plane $y = 0$ as it can also be seen by direct inspection on the asymptotic relations (33b) and (34a).

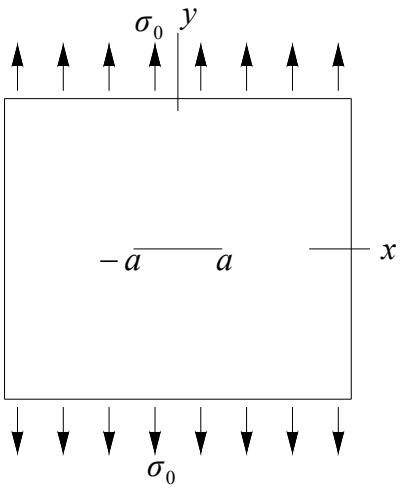

Fig. 2 Cracked body under remote tension in plane strain.

The solution to the original boundary value problem can be obtained by the superposition of two auxiliary problems. First, an un-cracked body of infinite extent subjected to boundary conditions (51) is examined. In that case, it can readily be verified that there are no gradient effects induced and thus the body is in a state of pure tension. In the second auxiliary problem, we consider a body with the same configuration as the original cracked body but with no remote loading now. The only loading applied is along the crack faces. This consists of equal and opposite tractions to those generated in the un-cracked body of the first auxiliary problem. In this case, Eqs. (49) and (50) still hold, whereas the boundary conditions along the faces of the crack are written as

$$t_{yy}(x,0)=-\sigma_0 \ , \quad m_{yyx}(x,0)=0 \qquad \text{for } |x|<a \ . \tag{52a,b}$$

Our intention now is to solve the second auxiliary problem described by the boundary conditions (49), (50) and (52).

In order to derive the integral equations for the mode I case, we define two functions that are analogous to the so-called *densities* utilized in the Distributed Dislocation Technique (e.g. Hills et al., 1996; Gourgiotis and Georgiadis, 2007; 2008). In the present case, we are led to the introduction of these functions by considering compatibility and the kinematical boundary condition in (50). The 'densities' $\varphi(x)$ and $\psi(x)$ are defined as

$$\varphi(x)=\partial u_y\left(x,0^+\right)\big/\partial x \ , \quad \psi(x)=\partial u_x\left(x,0^+\right)\big/\partial y \ . \tag{53a,b}$$

Of course, the latter functions are yet unknown, but we will soon formulate a system of coupled integral equations for them. To this end, we first note that the symmetry conditions in (50) imply

$$\varphi(x)=0 \ , \quad \psi(x)=0 \qquad \text{for } |x|\geq a \ . \tag{54a,b}$$

Moreover, the following closure conditions must be satisfied

$$\int_{-a}^{a}\varphi(x)\,dx=0 \ , \quad \int_{-a}^{a}\psi(x)dx=0 \ , \tag{55a,b}$$

where the first is to be imposed due to compatibility and the second due to the symmetry of the mode I problem w.r.t. the plane $x=0$ ($\psi(x)$ is an odd function).

The Fourier transforms of the 'densities' are written in terms of the transformed displacements as

$$\varphi^*(\xi)=-\mathrm{i}\xi u_y^*(\xi,0) \ , \quad \psi^*(\xi)=du_x^*(\xi,0)\big/dy \ , \tag{56a,b}$$

where $\varphi^*(\xi)=(2\pi)^{-1/2}\int_{-a}^{a}\varphi(t)e^{it\xi}dt$ and $\psi^*(\xi)=(2\pi)^{-1/2}\int_{-a}^{a}\psi(t)e^{it\xi}dt$ by virtue of (54).

Next, by using (43), (49) and (56), we write the functions $C_b(\xi)$ in terms of $\varphi(x)$ and $\psi(x)$

$$C_1(\xi)=-\frac{ic\xi\left(\nu+c\xi^2\right)}{(2\pi)^{1/2}(1-\nu)}\int_{-a}^{a}\left[\varphi(t)+\psi(t)\right]e^{it\xi}dt+\frac{i}{(2\pi)^{1/2}\xi}\int_{-a}^{a}\varphi(t)e^{it\xi}dt\ , \tag{57a}$$

$$C_2(\xi)=\frac{ic\,\mathrm{sgn}(\xi)}{2(2\pi)^{1/2}(1-\nu)}\int_{-a}^{a}\left[\beta^2\varphi(t)+\xi^2\psi(t)\right]e^{it\xi}dt\ , \tag{57b}$$

$$C_3(\xi)=\frac{ic\xi\left(\nu+c\xi^2\right)}{(2\pi)^{1/2}(1-\nu)}\int_{-a}^{a}\left[\varphi(t)+\psi(t)\right]e^{it\xi}dt\ , \tag{57c}$$

$$C_4(\xi)=-\frac{c\beta\left(c\beta^2-\nu\right)}{(2\pi)^{1/2}(1-\nu)}\int_{-a}^{a}\left[\varphi(t)+\psi(t)\right]e^{it\xi}dt\ . \tag{57d}$$

Finally, replacing $C_b(\xi)$ into the integral expressions for the total stress t_{yy} and the dipolar stress m_{yyx} (i.e. into (45) and (47)), enforcing the boundary conditions (52) and rearranging the order of integration results in a system of coupled integral equations for the functions $\phi(t)$ and $\psi(t)$

$$\lim_{y\to0^+}\frac{\mu}{2\pi}\left[\int_{-a}^{a}\varphi(t)\cdot L_1\left((x-t),y\right)dt+\int_{-a}^{a}\psi(t)\cdot L_2\left((x-t),y\right)dt\right]=-\sigma_0\quad\text{for}\quad|x|<a\ , \tag{58}$$

$$\lim_{y\to0^+}\frac{\mu}{2\pi}\left[\int_{-a}^{a}\varphi(t)\cdot L_3\left((x-t),y\right)dt+\int_{-a}^{a}\psi(t)\cdot L_4\left((x-t),y\right)dt\right]=0\quad\text{for}\quad|x|<a\ . \tag{59}$$

The kernels $L_b\left((x-t),y\right)$ (with $b=1,2,3,4$) are defined in Appendix B. It is noted that when $c\to0$, the above system of integral equations degenerates into the single integral equation governing the mode I crack problem in classical elasticity.

Now, with the aid of asymptotic analysis, we split the kernels $L_b\left((x-t),y=0^+\right)$ into their singular and regular parts

$$L_1\left((x-t), y=0^+\right)=\frac{c\gamma_1}{(x-t)^3}-\frac{\gamma_2}{4(x-t)}+N_1(x-t)\ , \tag{60a}$$

$$L_2\left((x-t), y=0^+\right)=\frac{c\gamma_3}{(x-t)^3}-\frac{\gamma_3}{4(x-t)}+N_1(x-t)\ , \tag{60b}$$

$$L_3\left((x-t), y=0^+\right)=\frac{c\gamma_3}{2(x-t)^2}+\frac{\gamma_3}{4}\ln\frac{|x-t|}{c^{1/2}}+N_2(x-t)\ , \tag{60c}$$

$$L_4\left((x-t), y=0^+\right)=\frac{c\gamma_1}{2(x-t)^2}+\frac{\gamma_3}{4}\ln\frac{|x-t|}{c^{1/2}}+N_2(x-t)\ , \tag{60d}$$

where the regular kernels $N_1(x-t)$ and $N_2(x-t)$ involve modified Bessel functions of the second kind and are given in closed form in Appendix B. The constants $(\gamma_1,\gamma_2,\gamma_3)$ are defined in terms of the Poisson's ratio as

$$\gamma_1=\frac{7-4\nu}{1-\nu}\ ,\quad \gamma_2=\frac{11-4\nu}{1-\nu}\ ,\quad \gamma_3=\frac{3-4\nu}{1-\nu}\ . \tag{61}$$

In light of the above, the following system of hypersingular integral equations is finally obtained

$$\text{F.P.}\int_{-1}^{1}\frac{\hat{c}\left[\gamma_1\hat{\varphi}(\hat{t})+\gamma_3\hat{\psi}(\hat{t})\right]}{(\hat{x}-\hat{t})^3}d\hat{t}-\text{C.P.V.}\int_{-1}^{1}\frac{\left[\gamma_2\hat{\varphi}(\hat{t})+\gamma_3\hat{\psi}(\hat{t})\right]}{4(\hat{x}-\hat{t})}d\hat{t}$$
$$+\int_{-1}^{1}\left[\hat{\varphi}(\hat{t})+\hat{\psi}(\hat{t})\right]\cdot\hat{N}_1(a\hat{x}-a\hat{t})\,d\hat{t}=-\frac{2\pi\sigma_0}{\mu}\quad\text{for}\quad|\hat{x}|<1\ , \tag{62}$$

$$\text{F.P.}\int_{-1}^{1}\frac{\hat{c}\left[\gamma_3\hat{\varphi}(\hat{t})+\gamma_1\hat{\psi}(\hat{t})\right]}{2(\hat{x}-\hat{t})^2}d\hat{t}+\int_{-1}^{1}\frac{\gamma_3\left[\hat{\varphi}(\hat{t})+\hat{\psi}(\hat{t})\right]}{4}\cdot\ln\frac{|\hat{x}-\hat{t}|}{\hat{c}^{1/2}}d\hat{t}$$
$$+\int_{-1}^{1}\left[\hat{\varphi}(\hat{t})+\hat{\psi}(\hat{t})\right]\cdot\hat{N}_2(a\hat{x}-a\hat{t})\,d\hat{t}=0\quad\text{for}\quad|\hat{x}|<1\ , \tag{63}$$

where the dimensionless quantities $\hat{\varphi}(\hat{t})=\varphi(a\hat{t})$, $\hat{\psi}(\hat{t})=\psi(a\hat{t})$, $\hat{x}=x/a$, $\hat{t}=t/a$ and $\hat{c}^{1/2}=c^{1/2}/a$ have been used to obtain normalization over the interval $[-1,1]$. In the above equations, the symbols

F.P.$\int$ and C.P.V.$\int$ denote that the integrals should be understood in the *Hadamard finite-part* and *Cauchy principal-value* sense, respectively. Some references for these types of integrals are, e.g., Muskhelishvili (1953), Kaya and Erdogan (1987), Tsamasphyros and Dimou (1990), and Monegato (1994). We also note that the second integral in (63) is weakly (logarithmically) singular. Although a number of formulations of mixed boundary value problems resulting in a *single* hypersingular integral equation can be found in the literature (see e.g. Kaya and Erdogan, 1987; Martin, 1991; Chan et al., 2008), we are not aware of any formulation resulting in a *system* of coupled hypersingular integral equations. This reflects the complexity of the present boundary value problem.

Further, in view of the previous asymptotic results showing that the displacement components (u_x, u_y) behave as $r^{3/2}$ (r is the distance from the crack tip) along the crack, we write the density functions in (53) under the following forms

$$\hat{\varphi}\left(\hat{t}\right)=\sum_{n=0}^{\infty}F_n\,U_n\left(\hat{t}\right)\cdot\left(1-\hat{t}^2\right)^{1/2}\ ,\quad \hat{\psi}\left(\hat{t}\right)=\sum_{n=0}^{\infty}G_n\,U_n\left(\hat{t}\right)\cdot\left(1-\hat{t}^2\right)^{1/2}\ ,\qquad \left|\hat{t}\right|<1\ , \tag{64a,b}$$

where $U_n\left(\hat{t}\right)$ are the Chebyshev polynomials of the second kind (Abramowitz and Stegun, 1964).

In view of the above, the system of integral equations takes the following form

$$\hat{c}\sum_{n=0}^{\infty}\left[\gamma_1F_n+\gamma_3G_n\right]\times\text{F.P.}\int_{-1}^{1}\frac{U_n\left(\hat{t}\right)\left(1-\hat{t}^2\right)^{1/2}}{\left(\hat{x}-\hat{t}\right)^3}d\hat{t}-\frac{1}{4}\sum_{n=0}^{\infty}\left[\gamma_2F_n+\gamma_3G_n\right]\times\text{C.P.V.}\int_{-1}^{1}\frac{U_n\left(\hat{t}\right)\left(1-\hat{t}^2\right)^{1/2}}{\left(\hat{x}-\hat{t}\right)}d\hat{t}$$
$$+\sum_{n=0}^{\infty}\left[F_n+G_n\right]\cdot Q_n^{(1)}\left(\hat{x}\right)=-\frac{2\pi\sigma_0}{\mu}\qquad\text{for}\qquad\left|\hat{x}\right|<1\ , \tag{65}$$

$$\frac{\hat{c}}{2}\sum_{n=0}^{\infty}\left[\gamma_3F_n+\gamma_1G_n\right]\times\text{F.P.}\int_{-1}^{1}\frac{U_n\left(\hat{t}\right)\left(1-\hat{t}^2\right)^{1/2}}{\left(\hat{x}-\hat{t}\right)^2}d\hat{t}+\frac{\gamma_3}{4}\sum_{n=0}^{\infty}\left[F_n+G_n\right]\times\int_{-1}^{1}U_n\left(\hat{t}\right)\left(1-\hat{t}^2\right)^{1/2}\ln\frac{\left|\hat{x}-\hat{t}\right|}{\hat{c}^{1/2}}d\hat{t}$$
$$+\sum_{n=0}^{\infty}\left[F_n+G_n\right]\cdot Q_n^{(2)}\left(\hat{x}\right)=0\qquad\text{for}\qquad\left|\hat{x}\right|<1\ , \tag{66}$$

where $Q_n^{(b)}\left(\hat{x}\right)$ (with $b=1,2$) are two regular integrals defined as

$$Q_n^{(b)}\left(\hat{x}\right)\equiv\int_{-1}^{1}U_n\left(\hat{t}\right)\left(1-\hat{t}^2\right)^{1/2}\cdot\hat{N}_b\left(a\hat{x}-a\hat{t}\right)d\hat{t}\ ,\quad b=1,2\ . \tag{67}$$

These regular integrals can be computed with the standard Gauss-Chebyshev quadrature. Further, the singular integrals in (65) and (66) are computed in *closed form* in the finite-part sense (see Appendix C). It is also noted that due to the closure conditions in (55) the coefficients F_0 and G_0 in (64) are equal to zero.

In view of the above, the previous system takes the form

$$-\frac{\pi\hat{c}}{4(1-\hat{x}^2)}\sum_{n=1}^{\infty}\left[\gamma_1 F_n+\gamma_3 G_n\right]\cdot\left[\left(n^2+n\right)U_{n+1}(\hat{x})-\left(n^2+3n+2\right)U_{n-1}(\hat{x})\right]$$

$$-\frac{\pi}{4}\sum_{n=1}^{\infty}\left[\gamma_2 F_n+\gamma_3 G_n\right]\cdot T_{n+1}(\hat{x})+\sum_{n=1}^{\infty}\left[F_n+G_n\right]\cdot Q_n^{(1)}(\hat{x})=-\frac{2\pi\sigma_0}{\mu}\qquad\text{for}\quad|\hat{x}|<1\ ,\quad(68)$$

$$-\frac{\pi\hat{c}}{2}\sum_{n=1}^{\infty}\left[\gamma_3 F_n+\gamma_1 G_n\right]\cdot(n+1)U_n(\hat{x})+\frac{\pi\gamma_3}{8}\sum_{n=1}^{\infty}\left[F_n+G_n\right]\cdot\left[\frac{T_{n+2}(\hat{x})}{n+2}-\frac{T_n(\hat{x})}{n}\right]$$

$$+\sum_{n=1}^{\infty}\left[F_n+G_n\right]\cdot Q_n^{(2)}(\hat{x})=0\qquad\text{for}\qquad|\hat{x}|<1\ ,\qquad(69)$$

where $T_n(\hat{x})$ are the Chebyshev polynomials of the first kind (Abramowitz and Stegun, 1964).

We solve numerically this system of functional equations using collocation points chosen as the roots of $T_{N+1}(\hat{x})$, viz. $\hat{x}_k=\cos\left[(2k-1)\pi/2(N+1)\right]$ with $k=1,2,...,N+1$. The $2N+2$ equations are solved in the *least-square* sense, to determine the $2N$ unknown coefficients F_n and G_n (with $n=1,2,3,...,N$) and, consequently, the functions $\varphi(\hat{x})$ and $\psi(\hat{x})$.

Figure 3a depicts the variation of the crack opening displacement (appropriately normalized). It is observed that the crack opening displacement in gradient elasticity takes on smaller values than the values according to classical elasticity. This stiffness effect becomes more pronounced with the increase of the material length $c^{1/2}$. In addition, Fig. 3b shows that the crack faces close more smoothly (cusp-like closure) as compared to the classical result.

Next, the total stress t_{yy} and the dipolar stress m_{yyx} will be determined ahead of the crack tips. A superposition of the solutions of the two auxiliary problems provides

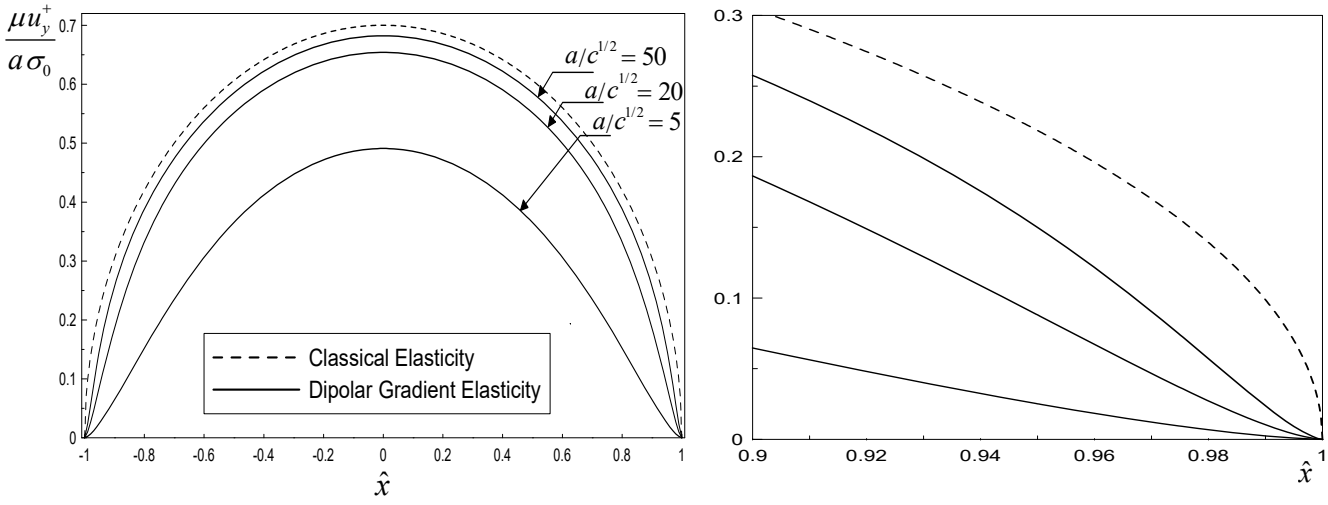

(a) (b)

Fig. 3 Profiles of the normalized crack opening displacement $(\mu u_y^+ / a\sigma_0)$ of the upper face (a) along the entire crack line, and (b) near to the RHS crack tip. The Poisson's ratio is $\nu = 0.3$.

$$t_{yy}\left(|x|>a, y=0^+\right)=\sigma_0+\frac{\mu c}{2\pi}\int_{-a}^{a}\frac{\left[\gamma_1\varphi(t)+\gamma_3\psi(t)\right]}{(x-t)^3}dt-\frac{\mu}{2\pi}\int_{-a}^{a}\frac{\left[\gamma_2\varphi(t)+\gamma_3\psi(t)\right]}{4(x-t)}dt$$
$$+\frac{\mu}{2\pi}\int_{-a}^{a}\left[\varphi(t)+\psi(t)\right]\cdot N_1(x-t)\,dt\ , \tag{70}$$

$$m_{yyx}\left(|x|>a,\ y=0^+\right)=\frac{\mu c}{2\pi}\int_{-a}^{a}\frac{\left[\gamma_3\varphi(t)+\gamma_1\psi(t)\right]}{2(x-t)^2}dt+\frac{\mu\gamma_3}{2\pi}\int_{-a}^{a}\frac{\left[\varphi(t)+\psi(t)\right]}{4}\cdot\ln\frac{|x-t|}{c^{1/2}}dt$$
$$+\frac{\mu}{2\pi}\int_{-a}^{a}\left[\varphi(t)+\psi(t)\right]\cdot N_2(x-t)\,dt\ , \tag{71}$$

where it is noted that the first two integrals in each of the above equations are not singular since $|x|>a$ now. Due to the symmetry of the problem with respect to y-axis, we confine attention only to the right crack tip. In order to evaluate the stresses, we utilize the results quoted in Appendix C (Eqs. (C5)-(C8)) for integrals involving Chebyshev polynomials.

Figure 4 depicts the distribution of the normal total stress ahead of the RHS crack tip for two different values of the ratio $a/c^{1/2}$. Normalized quantities are utilized and the new variable $\bar{x}=x-a$

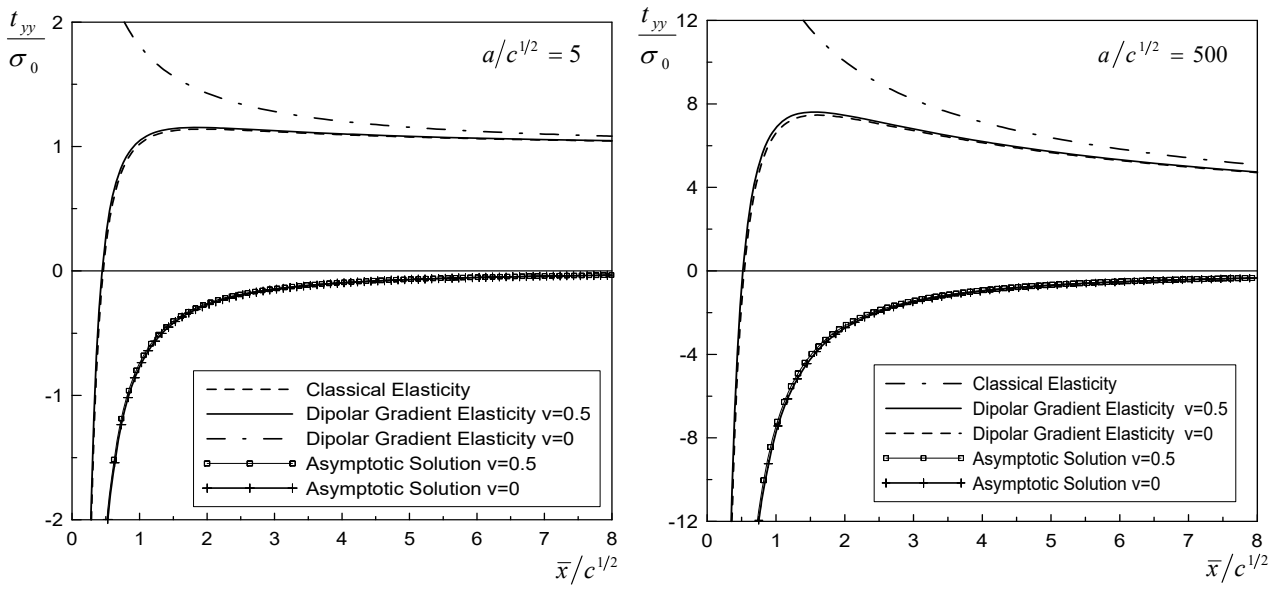

Fig. 4 Distribution of the total normal stress ahead of the crack tip for two different values of the ratio $a/c^{1/2}$ and for Poisson's ratios $\nu = 0$ and $\nu = 0.5$.

is introduced measuring distance from the RHS crack tip. The corresponding asymptotic fields in Section 4 and the classical solution are also shown in Figure 4. It is can readily be shown from (70) that, as $x \to a^+$ ($\hat{x} \to 1^+$), the total stress t_{yy} exhibits a singularity of the type $\bar{x}^{-3/2}$. This is in accord with our previous asymptotic result. Our results show that the asymptotic field is a good approximation of the full-field solution only within a distance from the crack-tip of $0.2c^{1/2}$ for $a/c^{1/2} = 5$, and $0.1c^{1/2}$ for $a/c^{1/2} = 500$. In the range shown in Fig. 4, the asymptotic total stress departs appreciably from the full-field solution. The behavior of t_{yy} reminds typical *boundary-layer* behavior as, e.g., that observed for the surface pressure near the leading edge of a Joukowski airfoil (van Dyke, 1964). We notice that for an initial zone in the crack-tip region the total normal stress t_{yy} takes on negative values exhibiting therefore a cohesive-traction character. This zone ranges from $0.45c^{1/2}$ to $0.5c^{1/2}$. Since c is of the order of $(0.1h)^2$, where $2h$ is the size of the unit cell, this zone is actually *extremely small* and perhaps can be ignored. This behavior was also observed before by Shi et al. (2000), Georgiadis (2003), and Wei (2006). Also, for $a \geq 5c^{1/2}$, t_{yy} exhibits a bounded maximum, whereas, for $a/c^{1/2} < 5$, no local maximum appears and the total stress tends

asymptotically to the limit of classical elasticity. We note, in addition, that at points lying outside the domain where the effects of microstructure are pronounced (roughly for $\bar{x} > 8c^{1/2}$), t_{yy} tends to the stress distribution given by the classical elasticity solution. Generally, the variation of the Poisson's ratio v has marginal effect on the total normal stress.

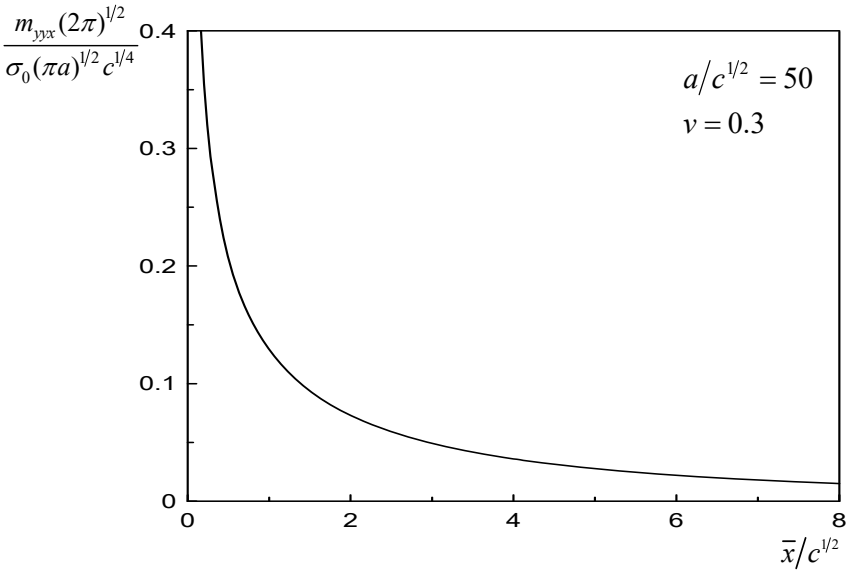

Fig. 5 Distribution of the dipolar stress ahead of the crack tip.

Further, from (71), we infer that the dipolar stress m_{yyx} behaves as $\bar{x}^{-1/2}$ in the vicinity of the crack tip. Again, this is in accord with the respective asymptotic result of Section 4. Figure 5 depicts the distribution of the dipolar stress ahead of the RHS crack tip. It is observed that the gradient effects are significant for $\bar{x} < 8c^{1/2}$, whereas, outside this zone, they gradually diminish to zero.

Finally, based on our previous analysis, we evaluate the normal strain ε_{yy} and the shear strain ε_{yx} along the crack line $y = 0^+$. In Fig. 6a the variation of the strain ε_{yy} is depicted. It is observed that the normal strain takes a finite value at the crack-tip ($\hat{x} = 1$), while the corresponding strain in classical elasticity exhibits a square root singularity. Also, it is shown that the effects of microstructure are more pronounced in the zone $|\bar{x}| < 5c^{1/2}$ (i.e. $0.9 < \hat{x} < 1.1$ in Fig. 6a), whereas outside this zone the distribution of the normal strain tends continuously to its classical counterpart. In Fig. 6b the distribution of the shear strain ε_{yx} is displayed. Contrary to the classical elasticity case,

the shear strain ε_{yx} is not zero at the crack-faces. Also, it is noted that as the ratio $a/c^{1/2}$ increases, the shear strain distribution converges pointwise to the classical solution.

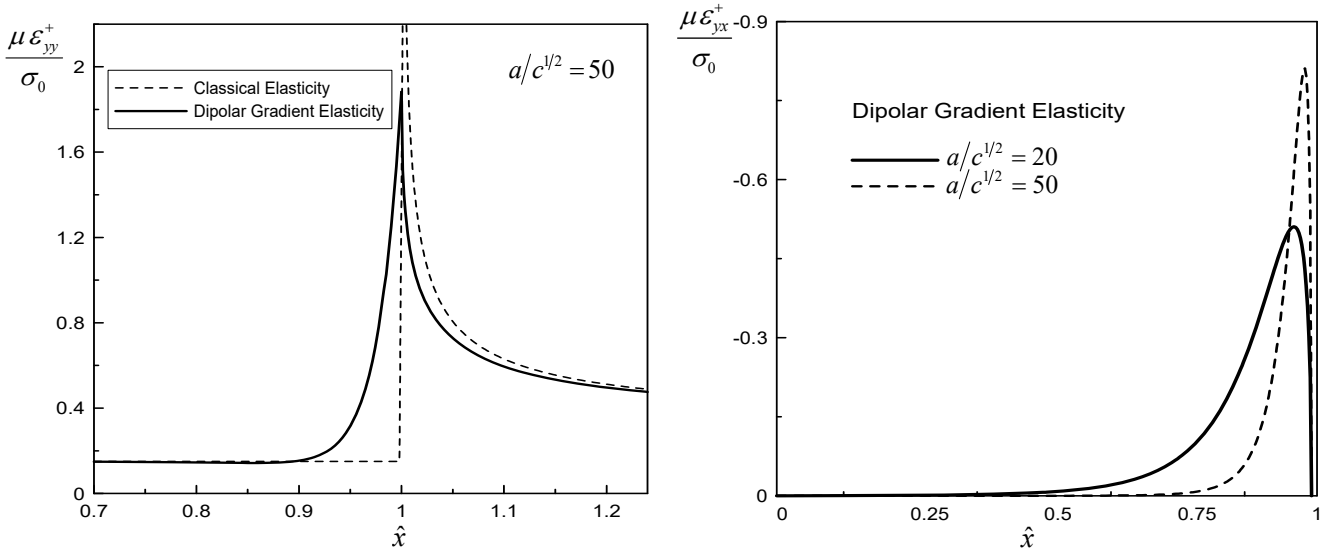

Fig. 6 Distribution of (a) the normal strain ε_{yy} and (b) the shear strain ε_{yx} of the upper crack face in classical and dipolar elasticity. The Poisson's ratio is $\nu = 0.3$.

5.2 Mode II crack

The problem of a mode II crack of length $2a$ (Fig. 7) is considered next. The crack faces are traction free and the body is considered to be in plane-strain conditions.

The following mixed boundary conditions hold for the upper half-plane ($y \geq 0$)

$$t_{yx}(x,0)=0\ ,\quad m_{yyy}(x,0)=0 \qquad \text{for}\ \ |x|<a\ , \tag{72a,b}$$

$$t_{yy}(x,0)=0\ ,\quad m_{yyx}(x,0)=0 \qquad \text{for}\ \ -\infty<x<\infty\ , \tag{73a,b}$$

$$u_x(x,0)=0\ ,\quad Du_y(x,0)\equiv\partial_y u_y(x,0)=0 \qquad \text{for}\ \ |x|>a\ , \tag{74a,b}$$

whereas the regularity conditions at infinity are

$$t_{yx}^{\infty}\to\tau_0\ ,\quad t_{yy}^{\infty},t_{xx}^{\infty}\to 0\ ,\quad m_{rpq}^{\infty}\to 0\ \ (r,p,q=x,y)\quad \text{as}\quad R\to\infty\ . \tag{75}$$

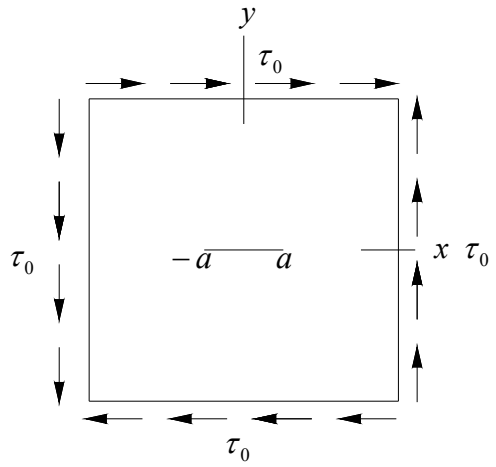

Fig. 7 Cracked body under remote shear in plane strain.

We note that the boundary conditions (73) are valid on the whole crack-line due to the antisymmetry of the mode II problem (c.f. the asymptotic relations (37b) and (38b)).

Since the procedure for the mode II problem is strictly analogous to that employed previously in the mode I case, we omit the details of the analysis and cite directly the results. The coupled system of hypersingular integral equations for the mode II case is obtained as

$$\text{F.P.}\int_{-1}^{1}\frac{\hat{c}\left[\kappa_1\hat{\zeta}\left(\hat{t}\right)-\kappa_3\hat{\eta}\left(\hat{t}\right)\right]}{\left(\hat{x}-\hat{t}\right)^3}d\hat{t}+\text{C.P.V.}\int_{-1}^{1}\frac{\kappa_3\hat{\eta}\left(\hat{t}\right)-\kappa_2\hat{\zeta}\left(\hat{t}\right)}{4\left(\hat{x}-\hat{t}\right)}d\hat{t}$$
$$+\int_{-1}^{1}\left[\hat{\zeta}\left(\hat{t}\right)\cdot\hat{M}_1\left(a\hat{x}-a\hat{t}\right)+\hat{\eta}\left(\hat{t}\right)\cdot\hat{M}_2\left(a\hat{x}-a\hat{t}\right)\right]d\hat{t}=-\frac{2\pi\tau_0}{\mu}\quad\text{for}\quad|\hat{x}|<1\,,\qquad(76)$$

$$\text{F.P.}\int_{-1}^{1}\frac{\hat{c}\left[\kappa_1\hat{\eta}\left(\hat{t}\right)-\kappa_3\hat{\zeta}\left(\hat{t}\right)\right]}{2\left(\hat{x}-\hat{t}\right)^2}d\hat{t}+\int_{-1}^{1}\frac{\kappa_4\hat{\eta}\left(\hat{t}\right)-\kappa_3\hat{\zeta}\left(\hat{t}\right)}{4}\cdot\ln\frac{\left|\hat{x}-\hat{t}\right|}{\hat{c}^{1/2}}d\hat{t}$$
$$+\int_{-1}^{1}\left[\hat{\zeta}\left(\hat{t}\right)\cdot\hat{M}_3\left(a\hat{x}-a\hat{t}\right)+\hat{\eta}\left(\hat{t}\right)\cdot\hat{M}_4\left(a\hat{x}-a\hat{t}\right)\right]d\hat{t}=0\quad\text{for}\quad|\hat{x}|<1\,,\qquad(77)$$

where the unknown ‘density’ functions are defined as

$$\zeta(x)=\partial u_x\left(x,0^+\right)/\partial x\,,\quad\eta(x)=\partial u_y\left(x,0^+\right)/\partial y\,,\qquad(78)$$

and satisfy the same symmetry and closure conditions as in (54) and (55). The regular kernels $M_b(x-t)$ (with $b=1,2,3,4$) involve modified Bessel functions of the second kind and are given in closed form in Appendix B. Further, the constants κ_b (with $b=1,2,3,4$) are given as

$$\kappa_1=\frac{8\nu^2-18\nu+9}{(1-\nu)(1-2\nu)}\ ,\quad \kappa_2=\frac{8\nu^2-22\nu+11}{(1-\nu)(1-2\nu)}\ ,\quad \kappa_3=\frac{8\nu^2-10\nu+1}{(1-\nu)(1-2\nu)}\ ,\quad \kappa_4=\frac{8\nu^2-14\nu+7}{(1-\nu)(1-2\nu)}\ . \quad (79)$$

The above system is solved numerically using the same collocation scheme as in the mode I case. In Figure 8, the variation of the tangential displacement along the crack-faces is depicted. Again, a cusp-like closure of the crack faces is observed.

The variation of the total shear stress t_{yx} ahead of the crack tip is displayed in Fig. 9. The corresponding asymptotic fields in Section 4 and the classical solution are also shown in Fig. 9. It is observed that the dependence on the Poisson's ratio of the total stress is stronger than in the mode I case. This dependence becomes more pronounced as the ratio $a/c^{1/2}$ increases. Also, the cohesive zone in the mode II case appears slightly larger than in mode I ranging from $0.56c^{1/2}$ (for $a/c^{1/2}=5$) to $0.77c^{1/2}$ (for $a/c^{1/2}=500$).

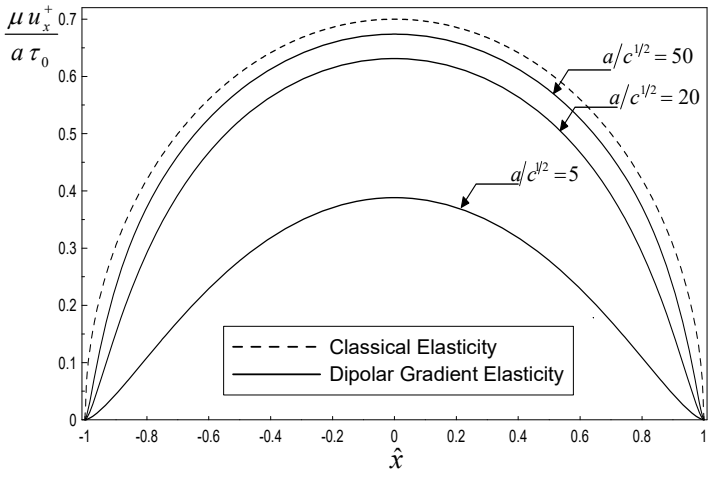

Fig. 8 Profiles of the normalized crack sliding displacement $(\mu u_x^+/a\tau_0)$ of the upper face along the entire crack line. The Poisson's ratio is $\nu=0.3$.

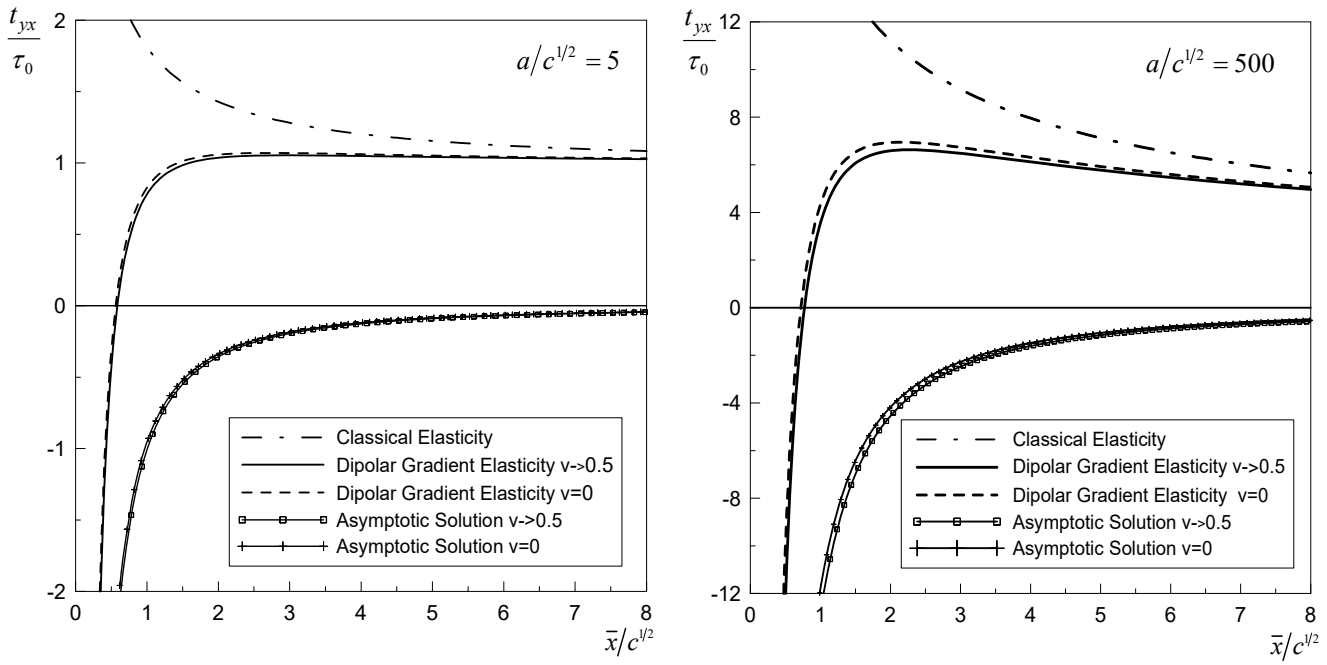

Fig. 9 Distribution of the total shear stress ahead of the crack tip for two different values of the ratio $a/c^{1/2}$ and for Poisson's ratios $\nu=0$ and $\nu=0.5$.

6. Evaluation of the *J*- integral

In this Section, we evaluate the J-integral of Fracture Mechanics in the mode I case and examine its dependence upon the ratio of lengths $c^{1/2}/a$ and the Poisson's ratio ν. In the works by Georgiadis and Grentzelou (2006), and Grentzelou and Georgiadis (2008), the expression given below for the J-integral was identified with the *energy release rate* at the crack tip in gradient elasticity and it was proved also that J is *path-independent* in the case of a quasi-static response and a homogeneous and isotropic material. The J-integral is defined in our case as

$$J=\int_{\Gamma}\left[Wn_x-P_q^{(n)}\frac{\partial u_q}{\partial x}-R_q^{(n)}D\left(\frac{\partial u_q}{\partial x}\right)\right]d\Gamma=\int_{\Gamma}\left(Wdy-\left[P_q^{(n)}\frac{\partial u_q}{\partial x}+R_q^{(n)}D\left(\frac{\partial u_q}{\partial x}\right)\right]d\Gamma\right), \quad (80)$$

where Γ is a piecewise, smooth, simple, two-dimensional contour in the (x,y)-plane surrounding the crack-tip. Also, $\mathbf{n}$ is the outward unit vector normal to Γ, W is the strain-energy density, u_q is

the displacement vector, and $(P_q^{(n)}, R_q^{(n)})$ are the auxiliary monopolar and dipolar tractions defined in Section 2.

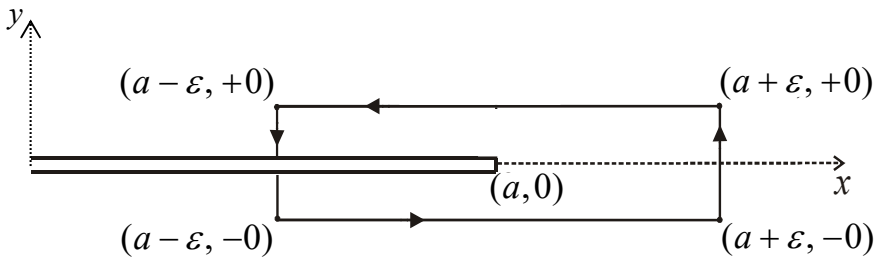

Fig. 10 Rectangular-shaped contour surrounding the RHS crack-tip.

For the evaluation of the J-integral, we consider as contour Γ a rectangular-shaped (surrounding the RHS crack-tip) with vanishing 'height' along the y-direction and with $\varepsilon \to +0$ (see Fig. 10). Such a contour was first introduced by Freund (1972) in examining the energy flux into the tip of a rapidly extending crack and it was proved particularly convenient in computing energy quantities in the vicinity of crack tips (see e.g. Burridge, 1976; Georgiadis, 2003; Gourgiotis and Georgiadis, 2008). In fact, this type of contour permits using solely the *asymptotic* near-tip stress and displacement fields. It is noted that upon this choice of contour, the integral $\int_\Gamma W\, dy$ in (80) becomes zero if we allow the 'height' of the rectangle to vanish. In this way, the expression for the J-integral becomes

$$J = -2 \lim_{\varepsilon \to +0} \left\{ \int_{a-\varepsilon}^{a+\varepsilon} \left(P_q^{(n)} \frac{\partial u_q}{\partial x} + R_q^{(n)} D\left(\frac{\partial u_q}{\partial x} \right) \right) dx \right\} . \tag{81}$$

For the mode I case, we take into account that the total shear stress t_{yx} and the dipolar stress m_{yyy} are zero along the crack line $\left(y = 0^+\right)$ and the crack-faces are defined by $\mathbf{n} = (0, \pm 1)$. Then, the J-integral assumes the following form

$$J=-2\lim_{\varepsilon\to+0}\left\{\int_{a-\varepsilon}^{a+\varepsilon}\left(t_{yy}\left(x,y=0^{+}\right)\cdot\frac{\partial u_{y}\left(x,y=0^{+}\right)}{\partial x}+m_{yyx}\left(x,y=0^{+}\right)\cdot\frac{\partial^{2}u_{x}\left(x,y=0^{+}\right)}{\partial x\partial y}\right)dx\right\}. \quad (82)$$

The dominant singular behavior (in the vicinity of the crack-tip) of the normal total stress t_{yy} is due to the hypersingular integral with the cubic singularity in (70), whereas for the dipolar stress m_{yyx} is due to the hypersingular integral with the square-type singularity in (71). These stresses are written as (see also Appendix C)

$$t_{yy}\left(x\to a^{+},y=0^{+}\right)=\lim_{x\to a^{+}}\frac{\mu c}{2\pi}\int_{-a}^{a}\frac{\left[\gamma_{1}\varphi\left(t\right)+\gamma_{3}\psi\left(t\right)\right]}{\left(x-t\right)^{3}}dt=$$

$$=\frac{2^{1/2}\mu\hat{c}}{16}\sum_{n=1}^{N}\left[\gamma_{1}F_{n}+\gamma_{3}G_{n}\right]\left(n+1\right)\cdot\left(\hat{x}-1\right)^{-3/2}\quad\text{for}\quad\hat{x}>1\,, \quad (83)$$

$$m_{yyx}\left(x\to a^{+},y=0^{+}\right)=\lim_{x\to a^{+}}\frac{\mu c}{2\pi}\int_{-a}^{a}\frac{\left[\gamma_{3}\varphi\left(t\right)+\gamma_{1}\psi\left(t\right)\right]}{2\left(x-t\right)^{2}}dt=$$

$$=a\frac{2^{1/2}\mu\hat{c}}{8}\sum_{n=1}^{N}\left[\gamma_{3}F_{n}+\gamma_{1}G_{n}\right]\left(n+1\right)\cdot\left(\hat{x}-1\right)^{-1/2}\quad\text{for}\quad\hat{x}>1\,. \quad (84)$$

Also, in view of the forms for $\hat{\varphi}\left(\hat{t}\right)$ and $\hat{\psi}\left(\hat{t}\right)$ in (64), the following asymptotic results are established for $\hat{x}\to1^{-}$

$$\frac{\partial u_{y}\left(x\to a^{-},y=0^{+}\right)}{\partial x}=\lim_{\hat{x}\to1^{-}}\sum_{n=1}^{N}F_{n}U_{n}\left(\hat{x}\right)\cdot\left(1-\hat{x}^{2}\right)^{1/2}$$

$$=2^{1/2}\sum_{n=1}^{N}F_{n}\left(n+1\right)\cdot\left(1-\hat{x}\right)^{1/2}\quad\text{for}\quad\hat{x}<1, \quad (85)$$

$$\frac{\partial^{2}u_{x}\left(x\to a^{-},y=0^{+}\right)}{\partial x\partial y}=\lim_{\hat{x}\to1^{-}}\frac{1}{a}\frac{\partial}{\partial\hat{x}}\left[\sum_{n=1}^{N}G_{n}U_{n}\left(\hat{x}\right)\cdot\left(1-\hat{x}^{2}\right)^{1/2}\right]$$

$$=-\frac{1}{2^{1/2}a}\sum_{n=1}^{N}G_{n}\left(n+1\right)\cdot\left(1-\hat{x}\right)^{-1/2}\quad\text{for}\quad\hat{x}<1. \quad (86)$$

Then, the above results allow us to write the J-integral under the form

$$J=-a\frac{\mu\hat{c}}{4}\lim_{\varepsilon\to 0}\left[\Lambda_1\cdot\int_{-(\varepsilon/a)}^{(\varepsilon/a)}\left(x_+\right)^{-3/2}\cdot\left(x_-\right)^{1/2}d\bar{x}-\Lambda_2\cdot\int_{-(\varepsilon/a)}^{(\varepsilon/a)}\left(x_+\right)^{-1/2}\cdot\left(x_-\right)^{-1/2}d\bar{x}\right]$$

$$=a\frac{\pi\mu\hat{c}}{8}\left[\Lambda_1+\Lambda_2\right], \qquad (87)$$

where

$$\Lambda_1=\sum_{n=1}^{N}\left(1+n\right)\left(\gamma_1F_n+\gamma_3G_n\right)\times\sum_{n=1}^{N}\left(1+n\right)F_n,\ \Lambda_2=\sum_{n=1}^{N}\left(1+n\right)\left(\gamma_3F_n+\gamma_1G_n\right)\times\sum_{n=1}^{N}\left(1+n\right)G_n. \qquad (88)$$

Also, $\bar{x}=\hat{x}-1$ and, for any real λ with the exception of $\lambda=-1,-2,-3,\ldots$, the following definitions of the distributions (of the *bisection* type) x_+^{λ} and x_-^{λ} are employed (see e.g. Gelfand and Shilov, 1964)

$$x_+^{\lambda}=\begin{cases}\left|\bar{x}\right|^{\lambda}, & \text{for } \bar{x}>0\\ 0, & \text{for } \bar{x}<0\end{cases} \quad \text{and} \quad x_-^{\lambda}=\begin{cases}0, & \text{for } \bar{x}>0\\ \left|\bar{x}\right|^{\lambda}, & \text{for } \bar{x}<0\end{cases}. \qquad (89)$$

It is further noted that the product of distributions inside the integrals in (87) is obtained here by the use of Fisher's theorem (Fisher, 1971), i.e. the operational relation $\left(x_+\right)^{-1-\lambda}\left(x_-\right)^{\lambda}=-\pi\,\delta(\bar{x})\left[2\sin(\pi\lambda)\right]^{-1}$ with $\lambda\neq -1,-2,-3,\ldots$ and $\delta(\bar{x})$ being the Dirac delta distribution. Use is also made of the fundamental property of the Dirac delta distribution that $\int_{-\varepsilon}^{\varepsilon}\delta(\bar{x})\,d\bar{x}=1$.

Our results are shown in the graph of Figure 11. The graph depicts the dependence of the ratio $J/J^{clas.}$ upon the ratio of lengths $c^{1/2}/a$ for three different values of the Poisson's ratio of the material. $J^{clas.}\equiv\pi(1-\nu^2)\sigma_0^2a/E$ is the respective value within the classical linear elastic fracture mechanics (see e.g. Rice, 1968). Our results show that as $c^{1/2}/a\to 0$, the J-integral in dipolar gradient elasticity tends continuously to its counterpart in classical elasticity. For $c^{1/2}\neq 0$, a decrease of the values of J is noticed in comparison with the classical theory and this indicates that the

rigidity effect *dominates* over the stress aggravation effect in the energy release rate. The ratio $J/J^{clas.}$ decreases monotonically with increasing values of $c^{1/2}/a$. This finding shows that the gradient theory predicts a strengthening effect since a reduction of the crack driving force takes place as the material microstructure becomes more pronounced.

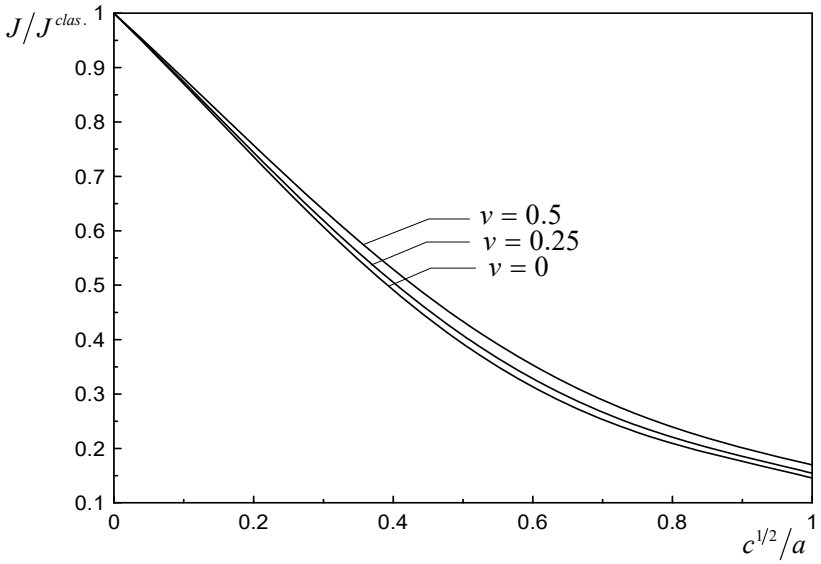

Fig. 11 Variation of the J-integral for the mode I case in dipolar gradient elasticity with $c^{1/2}/a$.

7. Conclusions

The present work is concerned with the full-field solutions of plane-strain problems of finite-length cracks in the framework of gradient elasticity. Form II of Mindlin's (1964) theory is employed with one characteristic length. The boundary value problems are attacked initially by the asymptotic Knein-Williams technique and then by an analytical / numerical technique based on hypersingular integral equations.

Our results show significant departure from the predictions of classical fracture mechanics. In particular, we found that a cracked solid governed by gradient elasticity behaves in a more rigid way (having increased stiffness) as compared to a solid governed by classical elasticity. Indeed, the crack-face displacements exhibit a cusp-like closure and the strain field is bounded at the crack-tip vicinity. On the other hand, the total stress ahead of the crack tip exhibits a typical boundary-layer

behavior with an initial very small area, adjacent to the crack tip, of cohesive tractions, the tractions then taking on positive values and reaching a bounded maximum. The length of the cohesive-traction area is extremely small. In addition, the J-integral in gradient elasticity tends continuously to its counterpart in classical elasticity as $c^{1/2}/a \to 0$, where $c^{1/2}$ is the material length and a is the half of the crack length. For $c^{1/2} \neq 0$, a decrease of its value is noticed in comparison with the classical theory and this indicates that the rigidity effect dominates over the stress aggravation effect in the energy release rate. The ratio $J/J^{clas.}$, where $J^{clas.}$ is the expression of the J-integral in classical elastic fracture mechanics, decreases monotonically with increasing values of $c^{1/2}/a$. This finding shows that the gradient theory predicts a strengthening effect since a reduction of the crack driving force takes place as the material microstructure becomes more pronounced.

Acknowledgement

The authors acknowledge with thanks support from the 'ΠΕΒΕ 2008' programme of NTU Athens (# 65/1695, title of the individual project: 'Fracture, contact and wave propagation problems in dipolar gradient elasticity'). Also, the authors are grateful to the anonymous reviewers of the paper for their very helpful comments.

Appendix A:

In this Appendix, we derive the total stresses and the equilibrium equations in polar coordinates.

The boundary condition (6) can be written in *direct* form as

$$\mathbf{P^{(n)}} = \mathbf{n}\cdot(\boldsymbol{\tau} - \nabla\cdot\mathbf{m}) - \overset{s}{\nabla}\cdot(\mathbf{n}\cdot\mathbf{m}) + (\overset{s}{\nabla}\cdot\mathbf{n})(\mathbf{nn}:\mathbf{m}) \ , \tag{A1}$$

where $\overset{s}{\nabla} = (\mathbf{I} - \mathbf{nn})\cdot\nabla$ is the surface gradient operator, $\mathbf{I}$ is the unit dyadic and ∇ is the usual gradient operator defined through the relation $\nabla(\,) = \mathbf{e}_r\,\partial_r(\,) + \mathbf{e}_\theta\, r^{-1}\,\partial_\theta(\,)$ in polar coordinates. In our case, where $\mathbf{n} = \mathbf{e}_\theta$, the surface gradient operator takes the form $\overset{s}{\nabla}(\,) = \mathbf{e}_r\partial_r(\,)$.

Further, the monopolar and dipolar stress tensors in the case of plane strain are written as

$$\boldsymbol{\tau} = \tau_{rr}\,\mathbf{e}_r \otimes \mathbf{e}_r + \tau_{\theta r}\,\mathbf{e}_\theta \otimes \mathbf{e}_r + \tau_{r\theta}\,\mathbf{e}_r \otimes \mathbf{e}_\theta + \tau_{\theta\theta}\,\mathbf{e}_\theta \otimes \mathbf{e}_\theta + \tau_{zz}\,\mathbf{e}_z \otimes \mathbf{e}_z \ , \tag{A2}$$

$$\begin{aligned}\mathbf{m} = {} & m_{rrr}\,\mathbf{e}_r \otimes \mathbf{e}_r \otimes \mathbf{e}_r + m_{r\theta r}\,\mathbf{e}_r \otimes \mathbf{e}_\theta \otimes \mathbf{e}_r + m_{rr\theta}\,\mathbf{e}_r \otimes \mathbf{e}_r \otimes \mathbf{e}_\theta + m_{r\theta\theta}\,\mathbf{e}_r \otimes \mathbf{e}_\theta \otimes \mathbf{e}_\theta \\ & + m_{\theta\theta\theta}\,\mathbf{e}_\theta \otimes \mathbf{e}_\theta \otimes \mathbf{e}_\theta + m_{\theta rr}\,\mathbf{e}_\theta \otimes \mathbf{e}_r \otimes \mathbf{e}_r + m_{\theta r\theta}\,\mathbf{e}_\theta \otimes \mathbf{e}_r \otimes \mathbf{e}_\theta + m_{\theta\theta r}\,\mathbf{e}_\theta \otimes \mathbf{e}_\theta \otimes \mathbf{e}_r \\ & + m_{\theta zz}\,\mathbf{e}_\theta \otimes \mathbf{e}_z \otimes \mathbf{e}_z + m_{zrz}\,\mathbf{e}_z \otimes \mathbf{e}_r \otimes \mathbf{e}_z + m_{rzz}\,\mathbf{e}_r \otimes \mathbf{e}_z \otimes \mathbf{e}_z + m_{zzr}\,\mathbf{e}_z \otimes \mathbf{e}_z \otimes \mathbf{e}_r \\ & + m_{z\theta z}\,\mathbf{e}_z \otimes \mathbf{e}_\theta \otimes \mathbf{e}_z + m_{zz\theta}\,\mathbf{e}_z \otimes \mathbf{e}_z \otimes \mathbf{e}_\theta \ .\end{aligned} \tag{A3}$$

Also, taking into account that the base vectors are related through the differential relations $\partial_\theta \mathbf{e}_r = \mathbf{e}_\theta$, $\partial_\theta \mathbf{e}_\theta = -\mathbf{e}_r$, $\partial_r \mathbf{e}_r = 0$, $\partial_r \mathbf{e}_\theta = 0$, we obtain

$$\mathbf{n}\cdot\mathbf{m} = m_{\theta rr}\,\mathbf{e}_r \otimes \mathbf{e}_r + m_{\theta r\theta}\,\mathbf{e}_r \otimes \mathbf{e}_\theta + m_{\theta\theta r}\,\mathbf{e}_\theta \otimes \mathbf{e}_r + m_{\theta\theta\theta}\,\mathbf{e}_\theta \otimes \mathbf{e}_\theta + m_{\theta zz}\,\mathbf{e}_z \otimes \mathbf{e}_z \ , \tag{A4}$$

$$\begin{aligned}\mathbf{n}\cdot(\boldsymbol{\nabla}\cdot\mathbf{m}) = {} & \left[\partial_r m_{r\theta r} + \frac{1}{r}\partial_\theta m_{\theta\theta r} + \frac{1}{r}m_{\theta rr} - \frac{1}{r}m_{\theta\theta\theta} + \frac{1}{r}m_{r\theta r}\right]\mathbf{e}_r \\ & + \left[\partial_r m_{r\theta\theta} + \frac{1}{r}\partial_\theta m_{\theta\theta\theta} + \frac{1}{r}m_{r\theta\theta} + \frac{1}{r}m_{\theta r\theta} + \frac{1}{r}m_{\theta\theta r}\right]\mathbf{e}_\theta \ ,\end{aligned} \tag{A5}$$

$$\overset{\mathbf{s}}{\boldsymbol{\nabla}}\cdot(\mathbf{n}\cdot\mathbf{m}) = \partial_r m_{\theta rr}\mathbf{e}_r + \partial_r m_{\theta r\theta}\mathbf{e}_\theta \ , \tag{A6}$$

$$\overset{\mathbf{s}}{\boldsymbol{\nabla}}\cdot\mathbf{n} = 0 \ . \tag{A7}$$

In view of the above, we are able to write for the total stresses Eqs. (17) and (18) of the main text.

Now as for the equations of equilibrium in terms of displacements, these are written in direct form as

$$\left(1 - c\nabla^2\right)\left[(1-2\nu)\nabla^2\mathbf{u} + \boldsymbol{\nabla}\left(\boldsymbol{\nabla}\cdot\mathbf{u}\right)\right] = 0 \ . \tag{A8}$$

In polar coordinates, (A8) becomes

$$\begin{aligned}&\left(1 - c\nabla^2\right)\left[s_r\mathbf{e}_r + s_\theta\mathbf{e}_\theta\right] = 0 \quad \Rightarrow \\ &\Rightarrow \quad \left[s_r - c[\nabla^2 s_r - r^{-2}s_r - 2r^{-2}\partial_\theta s_\theta]\right]\mathbf{e}_r + \left[s_\theta - c[\nabla^2 s_\theta - r^{-2}s_\theta + 2r^{-2}\partial_\theta s_r]\right]\mathbf{e}_\theta = 0 \ ,\end{aligned} \tag{A9}$$

with s_r and s_θ being given in Eqs. (21) of the main text. Then, from (A9) one readily obtains Eqs. (20) in the main body of the paper.

Appendix B:

In this Appendix, the kernels of the integral equations are derived in closed form.

Mode I case

The kernels $L_b\left((x-t),y\right)$ (with $b=1,2,3,4$) are defined as follows

$$L_b\left((x-t),y\right)=\int_{-\infty}^{\infty}k_b(\xi,y)e^{-\mathrm{i}\xi(x-t)}\,d\xi \quad , \tag{B1}$$

where

$$k_1(\xi,y)=\frac{\mathrm{i}c^2\beta^4\,\mathrm{sgn}(\xi)\left(2c\xi^2-1-y|\xi|\right)}{1-\nu}e^{-|\xi|y}-\mathrm{i}c\beta\xi\left[1+\frac{2(c\beta\xi)^2}{1-\nu}\right]e^{-y\beta} \quad , \tag{B2}$$

$$k_2(\xi,y)=\frac{\mathrm{i}c^2\beta^2\left(1+2c\xi^2-y|\xi|\right)\xi|\xi|}{1-\nu}e^{-|\xi|y}-\mathrm{i}c\beta\xi\left[1+\frac{2(c\beta\xi)^2}{1-\nu}\right]e^{-y\beta} \quad , \tag{B3}$$

$$k_3(\xi,y)=\frac{c^2\beta^2|\xi|\left(1+2c\xi^2-y|\xi|\right)}{1-\nu}e^{-|\xi|y}-c\beta\left[1+\frac{2(c\beta\xi)^2}{1-\nu}\right]e^{-y\beta}, \tag{B4}$$

$$k_4(\xi,y)=\frac{c^2\xi^2|\xi|\left(3+2c\xi^2-y|\xi|\right)}{1-\nu}e^{-y|\xi|}-c\beta\left[1+\frac{2(c\beta\xi)^2}{1-\nu}\right]e^{-y\beta} \quad . \tag{B5}$$

The above expressions are useful for the derivation of the field quantities *away* from the crack-axis (i.e. for $y\neq 0$). The kernels $L_b\left((x-t),y\right)$ are given in the thesis by Gourgiotis (2009).

With the aid of asymptotic analysis, the regular parts of the kernels $L_b\left((x-t),y=0^+\right)$ are given as

$$N_1(\rho)=-\frac{2}{(1-\nu)}\left\{\frac{1440c^3}{\rho^7}-\frac{72c^2}{\rho^5}+\frac{(7-4\nu)c}{2\rho^3}-\frac{3-4\nu}{8\rho}-\frac{(1-\nu)K_2\left(|\rho|/c^{1/2}\right)}{\rho}\right.$$
$$\left.-\frac{1}{\rho}\left[K_4\left(|\rho|/c^{1/2}\right)\left(1+\frac{30c}{\rho^2}\right)-K_2\left(|\rho|/c^{1/2}\right)\right]\right\}, \qquad \text{(B6)}$$

$$N_2(\rho)=-\frac{2}{(1-\nu)}\left\{\frac{240c^3}{\rho^6}-\frac{18c^2}{\rho^4}+\frac{(7-4\nu)c}{4\rho^2}+\frac{3-4\nu}{8}\ln\left(|\rho|/c^{1/2}\right)\right.$$
$$-\frac{1}{16}\left[2K_0\left(|\rho|/c^{1/2}\right)-K_2\left(|\rho|/c^{1/2}\right)-2K_4\left(|\rho|/c^{1/2}\right)+K_6\left(|\rho|/c^{1/2}\right)\right]$$
$$\left.-\frac{(1-\nu)}{2}\left[K_2\left(|\rho|/c^{1/2}\right)-K_0\left(|\rho|/c^{1/2}\right)\right]\right\}, \qquad \text{(B7)}$$

where $\rho=x-t$ and $K_i\left(R/c^{1/2}\right)$ is the i^{th} order modified Bessel function of the second kind.

Further, to show that the kernels $N_b(\rho)$ (with $b=1,2$) are regular, we expand the latter in series as $\rho\to 0$ (with the aid of the symbolic program MAPLE)

$$\lim_{\rho\to 0}N_b(\rho)=\left(a_1+a_2\ln|\rho|\right)\cdot\rho+O\left(\rho^3\ln|\rho|\right), \qquad \text{(B8)}$$

where a_b (with $b=1,2$) are constants. Now, since $\lim_{\rho\to 0}\rho^n\cdot\ln|\rho|=0$ for $n>0$, it is concluded that the above kernels are regular.

Mode II case

The regular kernels $M_b(\rho)$ (with $b=1,2,3,4$) in (76) and (77) are given as

$$M_1(\rho)=\frac{4}{(1-\nu)}\left\{\frac{720c^3}{\rho^7}-\frac{60c^2}{\rho^5}-\frac{c\left(8\nu^2+14\nu-7\right)}{4(1-2\nu)\rho^3}+\frac{\left(8\nu^2-6\nu+3\right)}{16(1-2\nu)\rho}\right.$$
$$\left.-K_2\left(|\rho|/c^{1/2}\right)\left[\frac{360c^2}{\rho^5}+\frac{60c}{\rho^3}-\frac{(1-\nu)^2}{(1-2\nu)\rho}\right]+\frac{45c}{\rho^3}K_0\left(|\rho|/c^{1/2}\right)\right\}, \qquad \text{(B9)}$$

$$M_2(\rho)=-\frac{4}{(1-\nu)}\left\{\frac{720c^3}{\rho^7}-\frac{36c^2}{\rho^5}-\frac{c\left(8\nu^2-2\nu-3\right)}{4(1-2\nu)\rho^3}+\frac{\left(8\nu^2-10\nu+1\right)}{16(1-2\nu)\rho}\right.$$

$$+3K_0\left(|\rho|/c^{1/2}\right)\left[\frac{15c}{\rho^3}+\frac{1}{2\rho}\right]-3K_2\left(|\rho|/c^{1/2}\right)\left[\frac{120c^2}{\rho^5}+\frac{24c}{\rho^3}-\frac{2\nu^2+4\nu-3}{6(1-2\nu)\rho}\right]\Bigg\}, \tag{B10}$$

$$M_3(\rho)=-\frac{4}{(1-\nu)}\Bigg\{\frac{120c^3}{\rho^6}-\frac{9c^2}{\rho^4}-\frac{c\left(8\nu^2-2\nu-3\right)}{8(1-2\nu)\rho^2}-\frac{\left(8\nu^2-10\nu+1\right)}{16(1-2\nu)}\ln\left(|\rho|/c^{1/2}\right)$$

$$-K_2\left(|\rho|/c^{1/2}\right)\left[\frac{60c^2}{\rho^4}+\frac{21c}{2\rho^2}+\frac{\nu(1-\nu)}{2(1-2\nu)}\right]+K_0\left(|\rho|/c^{1/2}\right)\left[\frac{15c}{2\rho^2}+\frac{\nu(1-\nu)}{2(1-2\nu)}\right]\Bigg\}, \tag{B11}$$

$$M_4(\rho)=\frac{4}{(1-\nu)}\Bigg\{\frac{120c^3}{\rho^6}-\frac{3c^2}{\rho^4}-\frac{c\left(8\nu^2-18\nu+9\right)}{8(1-2\nu)\rho^2}-\frac{\left(8\nu^2-14\nu+7\right)}{16(1-2\nu)}\ln\left(|\rho|/c^{1/2}\right)$$

$$-K_2\left(|\rho|/c^{1/2}\right)\left[\frac{60c^2}{\rho^4}+\frac{27c}{2\rho^2}-\frac{\nu^2}{2(1-2\nu)}\right]+K_0\left(|\rho|/c^{1/2}\right)\left[\frac{15c}{2\rho^2}-\frac{\nu^2}{2(1-2\nu)}\right]\Bigg\}. \tag{B12}$$

Appendix C:

In the main body of the paper, we have utilized closed-form expressions for several integrals involving Chebyshev polynomials. In this Appendix, we present these expressions.

In the case $|x|<1$, the following integrals are singular or hypersingular. They are evaluated as

$$\int_{-1}^{1}U_n(t)\left(1-t^2\right)^{1/2}\ln|x-t|\,dt=\begin{cases}\dfrac{\pi}{4}T_2(x)-\dfrac{\pi}{2}\ln 2, & n=0\\ \dfrac{\pi}{2}\left(\dfrac{T_{n+2}(x)}{n+2}-\dfrac{T_n(x)}{n}\right), & n\geq 1\end{cases}, \tag{C1}$$

$$\text{C.P.V.}\int_{-1}^{1}\frac{U_n(t)\left(1-t^2\right)^{1/2}}{x-t}dt=\pi T_{n+1}(x), \qquad n\geq 0, \tag{C2}$$

$$\text{F.P.}\int_{-1}^{1}\frac{U_n(t)\left(1-t^2\right)^{1/2}}{(x-t)^2}dt=-\pi(n+1)U_n(x), \quad n\geq 0, \tag{C3}$$

$$\text{F.P.}\int_{-1}^{1}\frac{U_n(t)\left(1-t^2\right)^{1/2}}{(x-t)^3}dt=\begin{cases}0, & n=0\\ -\dfrac{\pi}{4\left(1-x^2\right)}\left[\left(n^2+n\right)U_{n+1}(x)-\left(n^2+3n+2\right)U_{n-1}(x)\right], & n\geq 1\end{cases}. \tag{C4}$$

The integrals (C2)-(C4) can be found in the works of Kaya and Erdogan (1987), and Chan et al. (2003).

In the case $|x|>1$, the following integrals are regular. They are evaluated as

$$\int_{-1}^{1} U_n(t)\left(1-t^2\right)^{1/2}\ln|x-t|\,dt =$$

$$= \begin{cases} \dfrac{\pi}{2}\left(x^2-|x|\left(x^2-1\right)^{1/2}+\ln\left(|x|+\left(x^2-1\right)^{1/2}\right)-\ln 2-\dfrac{1}{2}\right), & n=0 \\ -\dfrac{\pi}{2}x^{-n}\left(1+\dfrac{\left(x^2-1\right)^{1/2}}{|x|}\right)^{-n}\left[\dfrac{1}{n}-\dfrac{1}{(n+2)x^2}\left(1+\dfrac{\left(x^2-1\right)^{1/2}}{|x|}\right)^{-2}\right], & n\geq 1 \end{cases}, \qquad \text{(C5)}$$

$$\int_{-1}^{1}\frac{U_n(t)\left(1-t^2\right)^{1/2}}{x-t}\,dt=\pi\left(x-\operatorname{sgn}(x)\left(x^2-1\right)^{1/2}\right)^{n+1}, \qquad n\geq 0\ , \qquad \text{(C6)}$$

$$\int_{-1}^{1}\frac{U_n(t)\left(1-t^2\right)^{1/2}}{(x-t)^2}\,dt=-\pi(n+1)\left(1-\frac{|x|}{\left(x^2-1\right)^{1/2}}\right)\left(x-\operatorname{sgn}(x)\left(x^2-1\right)^{1/2}\right)^{n}, \qquad n\geq 0\ , \qquad \text{(C7)}$$

$$\int_{-1}^{1}\frac{U_n(t)\left(1-t^2\right)^{1/2}}{(x-t)^3}\,dt=\frac{\pi}{2}(n+1)\left(x-\operatorname{sgn}(x)\left(x^2-1\right)^{1/2}\right)^{n-1}\left[n\left(1-\frac{|x|}{\left(x^2-1\right)^{1/2}}\right)^2+\frac{|x|-\left(x^2-1\right)^{1/2}}{\left(x^2-1\right)^{3/2}}\right], \quad n\geq 0\ . \qquad \text{(C8)}$$

References

Abramowitz, M., Stegun, I.A., 1964. Handbook of Mathematical Functions. National Bureau of Standards, Appl. Math. Series 55.

Amanatidou, E., Aravas, N., 2002. Mixed finite element formulations of strain-gradient elasticity problems. Comput. Meth. Appl. Mech. Eng. 191, 1723-1751.

Anderson, T.L., 1995. Fracture Mechanics: Fundamentals and Applications. CRC Press, Boca Raton.

Aravas, N., Giannakopoulos, A.E., 2009. Plane asymptotic crack-tip solutions in gradient elasticity, submitted.

Barber, J.R., 1992. Elasticity. Kluwer, Academic Publishers, Dordrecht.

Begley, M.R., Hutchinson, J.W., 1998. The mechanics of size-dependent indentation. J. Mech. Phys. Solids 46, 2049-2068.

Bleustein, J.L., 1967. A note on the boundary conditions of Toupin's strain-gradient theory. Int. J. Solids Struct. 3, 1053-1057.

Brock, L.M., Georgiadis, H.G., 2000. Sliding contact with friction of a thermoelastic solid at subsonic, transonic and supersonic speeds. J. Therm. Stresses 23, 629-656.

Brock, L.M., Georgiadis, H.G., 2007. Multiple-zone sliding contact with friction on an anisotropic thermoelastic half-space. Int. J. Solids Struct. 44, 2820-2836.

Burridge, R, 1976. An influence function of the intensity factor in tensile fracture. Int. J. Eng. Sci. 14, 725-734.

Cauchy, A.L., 1851. Note sur l' equilibre et les mouvements vibratoires des corps solides. Comptes-Rendus Acad. Paris 32, 323-326.

Chan, Y.S., Fannjiang, A.C., Paulino, G.H., 2003. Integral equations with hypersingular kernels-theory and applications to fracture mechanics. Int. J. Eng. Sci. 41, 683-720.

Chen, J.Y., Huang, Y., Ortiz, M., 1998. Fracture analysis of cellular materials: A strain gradient model. J. Mech. Phys. Solids 46, 789-828.

Chen, J.Y., Wei, Y., Huang, Y., Hutchinson, J.W., Hwang, K.C., 1999. The crack tip fields in strain gradient plasticity: The asymptotic and numerical analyses. Eng. Fract. Mech. 64, 625-648.

Cleveringa, H.H.M., van der Giessen, E., Needleman, A., 2000. A discrete dislocation analysis of mode I crack growth. J. Mech. Phys. Solids 48, 1133–1157.

Cook, T.S., Weitsman, Y., 1966. Strain-gradient effects around spherical inclusions and cavities. Int. J. Solids Struct. 2, 393-406.

Elssner, G., Korn, D., Ruhle, M., 1994. The influence of interface impurities on fracture energy of UHV diffusion bonded metal-ceramic bicrystals. Scripta Metall. Mater. 31, 1037–1042.

Erdogan, F., 1978. Mixed boundary-value problems in mechanics. In: Nemat-Nasser S. (Ed.), Mechanics Today, Vol. 4, Academic Press, New York, pp. 1-86.

Eshel, N.N., Rosenfeld, G., 1970. Effects of strain-gradient on the stress-concentration at a cylindrical hole in a field of uniaxial tension. J. Eng. Math. 4, 97-111.

Fisher, B., 1971. The product of distributions. Q. J. Math. Oxford 22, 291-298.

Fleck, N.A., Muller, G.M., Ashby, M.F., Hutchinson, J.W., 1994. Strain gradient plasticity: theory and experiment. Acta Metall. Mater. 42, 475-487.

Fleck, N.A., Shu, J.Y., 1995. Microbuckle initiation in fibre composites: a finite element study. J. Mech. Phys. Solids 43, 1887-1918.

Fleck, N.A., Hutchinson, J.W., 1997. Strain gradient plasticity. In: Hutchinson, J.W., Wu, T.Y. (Eds.), Advances in Applied Mechanics, Vol. 33, Academic Press, New York, pp. 295-361.

Fleck, N.A., Hutchinson, J.W., 1998. A discussion of strain gradient plasticity theories and application to shear bands. In: de Borst, R., van der Giessen, E. (Eds.), Material Instabilities in Solids, Wiley, New York, pp. 507-519.

Freund, L.B., 1972. Energy flux into the tip of an extending crack in an elastic solid. J. Elast. 2, 341-349.

Gao, H., Huang, Y., Nix, W.D., Hutchinson, J.W., 1999. Mechanism-based strain gradient plasticity – I. Theory. J. Mech. Phys. Solids 47, 1239-1263.

Gazis, D.C., Herman, R., Wallis, R.F., 1960. Surface elastic waves in cubic crystals. Phys. Rev. 119, 533-544.

Gelfand, I.M., Shilov, G.E., 1964. Generalized Functions, Vol. 1, Academic Press, New York.

Georgiadis, H.G., Vardoulakis, I., Lykotrafitis, G., 2000. Torsional surface waves in a gradient-elastic half-space. Wave Motion 31, 333-348.

Georgiadis, H.G., 2003. The mode-III crack problem in microstructured solids governed by dipolar gradient elasticity: Static and dynamic analysis. ASME J. Appl. Mech. 70, 517-530.

Georgiadis, H.G., Vardoulakis, I., Velgaki, E.G., 2004. Dispersive Rayleigh-wave propagation in microstructured solids characterized by dipolar gradient elasticity. J. Elast. 74, 17-45.

Georgiadis, H.G., Grentzelou, C.G., 2006. Energy theorems and the *J*-integral in dipolar gradient elasticity. Int. J. Solids Struct. 43, 5690-5712.

Georgiadis, H.G., Anagnostou, D. 2008. Problems of the Flamant-Boussinesq and Kelvin type in dipolar gradient elasticity. J. Elast. 90, 71-98.

Germain, P., 1973. The method of virtual power in continuum mechanics. Part 2: microstructure. SIAM J. Appl. Math. 25, 556-575.

Giannakopoulos, A.E., Stamoulis, K., 2007. Structural analysis of gradient elastic components. Int. J. Solids Struct. 44, 3440-3451.

Grentzelou, C.G., Georgiadis, H.G., 2005. Uniqueness for plane crack problems in dipolar gradient elasticity and in couple-stress elasticity. Int. J. Solids Struct. 42, 6226-6244.

Grentzelou, C.G., Georgiadis, H.G., 2008. Balance laws and energy release rates for cracks in dipolar gradient elasticity. Int. J. Solids Struct. 45, 551–567.

Gourgiotis, P.A., Georgiadis, H.G., 2007. Distributed dislocation approach for cracks in couple-stress elasticity: shear modes. Int. J. Fract. 147, 83-102.

Gourgiotis, P.A., Georgiadis, H.G., 2008. An approach based on distributed dislocations and disclinations for crack problems in couple-stress elasticity. Int. J. Solids Struct. 45, 5521-5539.

Gourgiotis, P.A., 2009. Fracture and Dislocation Problems in Generalized Continuum Theories. Ph.D. Thesis, National Technical University of Athens.

Hills, D.A., Kelly, P.A., Dai, D.N., Korsunsky, A.M., 1996. Solution of Crack Problems: The Distributed Dislocation Technique. Kluwer Academic Publishers.

Huang, Y., Zhang, L., Guo, T.F., Hwang, K.C., 1997. Mixed mode near tip fields for cracks in materials with strain-gradient effects. J. Mech. Phys. Solids 45, 439-465.

Huang, Y., Chen, J.Y., Guo, T.F., Zhang, L., Hwang, K.C., 1999. Analytic and numerical studies on mode I and mode II fracture in elastic-plastic materials with strain gradient effects. Int. J. Fract. 100, 1-27.

Huang, Y., Gao, H., Nix, W.D., Hutchinson, J.W., 2000. Mechanism-based strain gradient plasticity – II. Analysis. J. Mech. Phys. Solids 48, 99-128.

Huang, Y., Qu, S., Hwang, K.C., Li, M., Gao, H., 2004. A conventional theory of mechanism-based strain gradient plasticity. Int. J. Plasticity 20, 753-782.

Hwang, K.C., Jiang, H., Huang, Y., Gao, H., Hu, N., 2002. A finite deformation theory of strain gradient plasticity. J. Mech. Phys. Solids 50, 81-99.

Kakunai, S., Masaki, J., Kuroda, R., Iwata, K., Nagata, R., 1985. Measurement of apparent Young's modulus in the bending of cantilever beam by heterodyne holographic interferometry. Exp. Mech. 21, 408-412.

Karlis, G.F., Tsinopoulos, S.V., Polyzos, D., Beskos, D.E., 2007. Boundary element analysis of mode I and mixed mode (I and II) crack problems of 2-D gradient elasticity. Comp. Meth. Appl. Mech. Eng. 196, 5092-5103.

Kaya, A.C., Erdogan, F., 1987. On the solution of integral equations with strongly singular kernels. Q. Appl. Math. XLV (1), 105–122.

Knein, M., 1927. Zur Theorie des Druckversuchs. Abhandlungen Aerodyn. Inst. T.H. Aachen 7, 43-62.

Knowles, J.K., Pucik, T.A., 1973. Uniqueness for plane crack problems in linear elastostatics. J. Elast. 3, 155-160.

Lakes, L., 1995. Experimental methods for study of Cosserat elastic solids and other generalized elastic continua. In: Muhlhaus, H.-B. (Ed.), Continuum Models for Materials with Microstructure, John Wiley and Sons, Chichester, pp. 1-25.

Lazar, M., Maugin, G.A., 2005. Nonsingular stress and strain fields of dislocations and disclinations in first strain gradient elasticity. Int. J. Engng. Sci. 43, 1157-1184.

Ma, Q., Clarke, D.S., 1995. Size dependent hardness in silver single crystals. J. Mater. Res. 10, 853-863.

Martin, P.A., 1991. End-point behavior of solutions to hypersingular integral equations. Proc. R. Soc. Lond. A 432, 301-320.

Mindlin, R.D., 1964. Micro-structure in linear elasticity. Arch. Ration. Mech. Anal. 16, 51-78.

Mindlin, R.D., Eshel, N.N., 1968. On first-gradient theories in linear elasticity. Int. J. Solids Struct. 4, 109-124.

Mindlin, R.D., Tiersten, H.F., 1962. Effects of couple-stresses in linear elasticity. Arch. Ration. Mech. Anal. 11, 415-448

Monegato, G., 1994. Numerical evaluation of hypersingular integrals. J. Comp. Appl. Math. 50, 9-31.

Muskhelishvili, N.I., 1958. Singular Integral Equations. Wolters-Noordhoff Publishing. Groningen.

Poole, W. J., Ashby, M. F., Fleck, N. A. 1996. Micro-hardness of annealed and work-hardened copper polycrystals. Scripta Mater. 34, 559-564.

Prakash, V., Freund, L.B., Clifton, R.J., 1992. Stress wave radiation from a crack tip during dynamic initiation. ASME J. Appl. Mech. 59, 356-365.

Radi, E., 2007. Effects of characteristic material lengths on mode III crack propagation in couple stress elastic-plastic materials. Int. J. Plast. 23, 1439-1456.

Radi, E., 2008. On the effects of characteristic lengths in bending and torsion on mode III crack in couple stress elasticity. Int. J. Solids Struct. 45, 3033-3058.

Rice, J.R., 1968. Mathematical analysis in the mechanics of fracture. In: Liebowitz, H. (Ed.), Fracture – An Advanced Treatise, Vol. 2, Academic Press, New York, pp. 191-311.

Shi, M.X., Huang, Y., Hwang, K.C., 2000. Fracture in the higher-order elastic continuum. J. Mech. Phys. Solids 48, 2513-2538.

Shu, J.Y., King, W.E., Fleck, N.A., 1999. Finite elements for materials with strain gradient effects. Int. J. Numer. Methods Eng. 44, 373-391.

Stolken, J.S., Evans, A.G., 1998. A microbend test method for measuring the plasticity length scale. Acta Mater. 46, 5109-5115.

Toupin, R.A., 1962. Perfectly elastic materials with couple stresses. Arch. Ration. Mech. Anal. 11, 385–414.

Tsamasphyros, G., Dimou, G., 1990. Gauss quadrature rules for finite part integrals. Int. J. Numer. Methods Eng. 30, 13-26.

Tsamasphyros, G.I., Markolefas, S., Tsouvalas, D.A., 2007. Convergence and performance of the h- and p-extensions with mixed finite element C^0-continuity formulations, for tension and buckling of a gradient elastic beam. Int. J. Solids Struct. 44, 5056-5074.

Tsepoura, K.G., Papargyri-Beskou, S., Polyzos, D., 2002. A boundary element method for solving 3D static gradient elastic problems with surface energy. Comput. Mech. 29, 361-381.

van Dyke, M., 1964. Perturbation Methods in Fluid Mechanics, Academic Press, New York.

Vardoulakis, I., Sulem, J., 1995. Bifurcation Analysis in Geomechanics. Blackie Academic and Professional (Chapman and Hall), London.

Vardoulakis, I., Georgiadis H.G., 1997. SH surface waves in a homogeneous gradient elastic half-space with surface energy. J. Elast. 47, 147-165.

Voigt, W., 1887. Theoretische Studien uber die Elasticitatsverhaltnisse der Krystalle. Abh. Ges. Wiss. Gottingen 34.

Wei, Y., Hutchinson, J.W., 1997. Steady-state crack growth and work of fracture for solids characterized by strain gradient plasticity. J. Mech. Phys. Solids 45, 1253-1273.

Wei, Y., 2006. A new finite element method for strain gradient theories and applications to fracture analyses. Eur. J. Mech. A/Solids 25, 897-913.

White, R.M., 1970. Surface elastic waves. Proceedings IEEE 58, 1238-1276.

Williams, M.L., 1952. Stress singularities resulting from various boundary conditions in angular corners of plates in extension. ASME J. Appl. Mech. 74, 526-528.

Zhang, L., Huang, Y., Chen, J.Y., Hwang, K.C., 1998. The mode-III full-field solution in elastic materials with strain gradient effects. Int. J. Fract. 92, 325-348.